Journal of Petroleum Science and Engineering 204 (2021) 108734

Contents lists available at ScienceDirect

Journal of Petroleum Science and Engineering

journal homepage: http://www.elsevier.com/locate/petrol

Study on waxy crudes characterisation and chemical inhibitor assessment

Nura Makwashi [a], Donglin Zhao [b,*], Mukhtar Abdulkadir [c], Tariq Ahmed [a], Ishaka Muhammad [d]

[a] Department of Chemical and Petroleum Engineering, Bayero University Kano, Nigeria
[b] Division of Chemical and Petroleum Engineering, London South Bank University, SE1 0AA, UK
[c] Department of Chemical Engineering, Federal University of Technology, Minna, Niger State, Nigeria
[d] Department of Chemistry, Zamfara State College of Education Maru, PMB, 1002, Nigeria

ARTICLE INFO

Keywords:
Wax inhibitor
Precipitation and deposition
Micro and macro crystalline wax

ABSTRACT

Wax deposition brings severe challenges to the production, transportation, and storage of crude oils. Accumulation of wax can block the pipeline, lead to equipment failure, and lose production. The use of chemical inhibitors has been reported as one of the most effective measures to mitigate wax deposition in the pipeline. The inhibition efficiency depends on the effects of the inhibitor molecules on the formation, growth, agglomeration and morphology of wax crystals. The chemicals and their compositions in the inhibitor together with the crude composition determine wax inhibition performance. Many different types of chemical inhibitors have been developed. Oil industry benefits significantly from high-efficiency inhibitors. This paper reported a simple method to optimise the inhibition performance by blending different inhibitors. Firstly, a comprehensive characterisation of two naturally waxy crude oils (KSG#49 and Ex Mwambe) and a synthetic crude oil was presented. The synthetic crude oil was prepared by mixing a dead oil of 3% wt wax content with a solid wax sample obtained from the North Sea field. The variation in properties of the three oils was evaluated through cloud point measurements, pour point, wax content, SARA fractions, colloidal instability index, American Petroleum Institute gravity (APIg), and the n-Paraffin distribution. Then, the influence of four Polymer-based pour point depressants (PPDs) on wax crystallization were critically assessed. The PPDs induced morphological changes to wax crystals transformed the needle-shaped crystals into an agglomerate. The small particles dispersed in the oil matrix reduced the apparent viscosity and wax gelling properties, and the efficiency of PPDs could be affected by the SARA fraction. A higher fraction of flocculated asphaltenes provides active sites for wax crystallization. Hence it increases cloud point and interferes with the crystal inhibition mechanism. Finally, a blended PPD produces a synergistic effect on inhibition performance that effectively reduces apparent viscosity, wax appearance temperature (WAT) and pour point (PP). The improvement can be attributed to the interactions between the molecules of wax inhibitors with wax crystals. This works sheds light on new inhibitor development by blending different inhibitors to promote performance synergies.

1. Introduction

Wax, also known as paraffin wax in crude oil, is one of the notorious pipe blockers, with asphaltene as the second molecules. The solubility of wax crystals is a function of temperature, whereas pressure hardly influences the solubility (Siljuberg, 2012). Below its melting point, the crystalline wax structure is formed either from their distinct compounds or from the combination of one another (Kasumu, 2014; Mozes, 1982). The crystals' shapes are predominantly orthorhombic unit cell, having a distribution of paraffin chain lengths ranging from C_{17}–C_{100}^{+} (Mozes, 1982). It is worth noting that as the temperature of the fluid drops wax crystals precipitation occur easily compared to other crude oil fractions (e.g Asphaltenes) (Bai and Zhang, 2013; Bai and Bai, 2005). The crystals are classified into two types (Hao et al., 2019; Lee, 2008; Li et al., 2018; Zheng et al., 2016); (i) macro-crystalline and (ii) micro-crystalline paraffin wax molecules. Paraffin wax composition has 80 to 90 percent macrocrystalline (Rehan et al., 2016). They are made up of low molecular weight straight-chain n-alkanes (C_{16} to C_{36}) that crystallizes in needle or platelet shape at low temperature (Lee, 2008; Li et al., 2018). They are usually found in the production and transportation systems (Al-Safran and Brill, 2017; Hao et al., 2019).

Micro-crystalline waxes are higher carbon number (C_{30} to C_{60}) molecules consisting of high fractions of branches and cycloalkanes.

* Corresponding author.
E-mail address: donglin.zhao@lsbu.ac.uk (D. Zhao).

https://doi.org/10.1016/j.petrol.2021.108734
Received 12 November 2020; Received in revised form 22 March 2021; Accepted 26 March 2021
Available online 31 March 2021

Acronyms

WAT = wax appearance temperature
GC/MS = gas chromatography coupled mass spectrometry
PPDs = pour point depressants
PP = Pour Point
TIC = total ion chromatogram
CII = Colloidal instability index
SARA = Saturates, Asphaltenes, Rasins and Aromatics
HTGC = High temperature gas chromatography

These complicated wax structures originate significant changes to the production, transportation, and storage of crude oils. Oil industries usually face severe issues regarding the inaccurate prediction of fluid flow behaviours that often lead to pipe blockage, equipment failure, and production loss. Therefore, accurate prediction of reservoir fluid's rheological behaviour and properties is paramount and still under scrutiny, particularly wax precipitation and deposition. Usually, this study comes at the early stage of oil field development before the front end engineering design (FEED) and after completing the conceptual design and the feasibility study (Cochran, 2003; de Oliveira et al., 2016). This is also known as the pre-deposition stage in wax deposition experimental study. Following this, the field engineers use some of the data to develop a wax intervention or mitigation strategies. For instance,

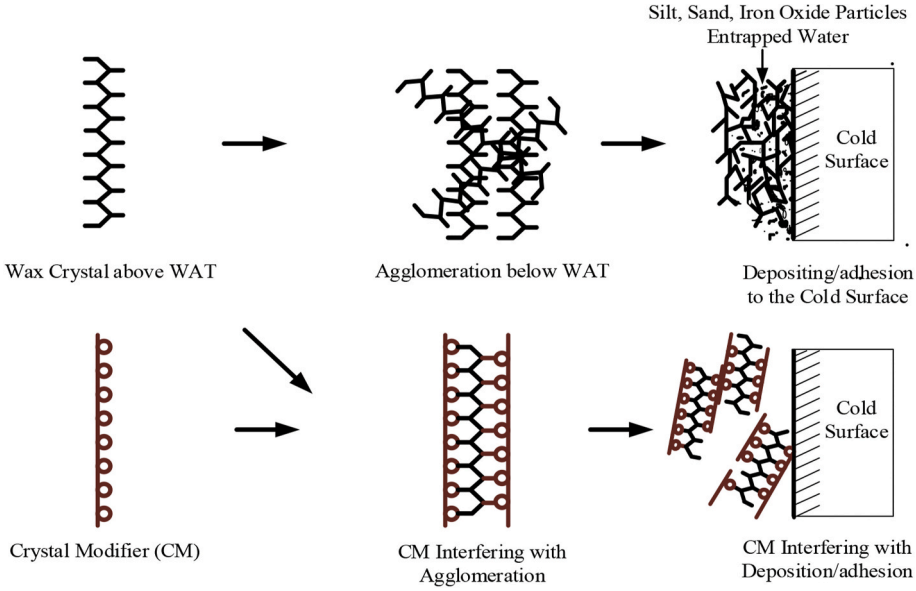

Fig. 1. Interaction mechanisms between wax crystals modifier with wax crystals (Adapted from Allen and Roberts, 1978, cited in Sousa et al., 2019 and Al-yaari, 2011).

Hence, it tends to have a higher crystallization temperature and usually precipitates in the form of needles and mal-crystalline shapes (Japper-Jaafar et al., 2016; Keeper, 2013; Kok and Saracoglu, 2000; Mansoori, 2009; Zheng et al., 2016). Microcrystalline is mostly found at the bottom of the sludge tanks (Al-Safran and Brill, 2017). Furthermore, small underdeveloped crystals with mal-crystalline shape frequently agglomerate under a fast cooling rate. Rapid cooling produces needle forms crystals, while slow crystallization favours the growth of the plate's shapes (Turner, 1971). In most cases, all these forms are usually produced in a single crystallization, although one of them often is predominant under a given set of conditions. Hence, in this paper, both the carbon chain (n-paraffin distribution) and the different crudes' morphology was investigated. The study is aimed to outline the basic structure and identify the region of macrocrystalline (C_{15} to C_{36}) and microcrystal ($>C_{36}$) paraffin wax in the samples.

The crystallization of wax occurs when the flowing fluid's temperature is less than or equal to the cloud point temperature or wax appearance temperature (WAT). In contrast, deposition is a term used to describe the formation and growth of a layer of the precipitated wax crystal on a surface (Hammami and Ratulowski, 2007; Yang et al., 2015). The main mechanisms responsible for wax precipitation include nucleation, growth and agglomeration (Yang et al., 2015; Zhu et al., 2008). These processes usually occur individually or concurrently, with one stage always being predominant at a time. During the later process, the interlock of wax crystals causes strong network formation in the system (Yang et al., 2015).

the wax deposition mitigation could be either by corrective or preventive methods (Al-yaari, 2011; Lee, 2008). The use of chemical inhibitors has been reported as one of the most effective oil industries' measures. However, the inhibitors' exact mechanisms interacting with wax crystals (Fig. 1)are still under scrutiny (Chi et al., 2016). Similarly, as of today, there is no universally accepted chemical inhibitor developed for all kind of crude oil due to their varying properties, and hence, chemical treatment is usually designed to fit the specific crude oil at a given environmental condition (Adeyanju and Oyekunle, 2014; Halim et al., 2011; Kang et al., 2014).

In reality, chemical inhibitors disrupted the order of aggregation of growing wax crystals, thereby influenced WAT, PP and viscosity as highlighted (Fig. 1). The inhibition performance improvement is indicated by the decrease of viscosity and delay in wax appearance temperature and pour point. However, some studies such as Pedersen and Rønningsen (2003), Wang et al. (2016), and Wu et al. (2012) have indicated an insignificant difference in WAT and PP in the presence of wax inhibitor. Whereas, studies by (Kelland, 2009; Wang et al., 2015, 2016) reported cases where WAT decreases with the addition of wax inhibitors – particularly at higher dosages (Perez et al., 2015). This suggests that the influence of wax inhibitors on the crude oil properties and morphology varies.

On the other hand, previous studies showed that SARA fractions significantly influence oil properties, including viscosity, wax crystallization and deposition (Fan and Buckley, 2002; Jewell et al., 1972) and even the inhibition mechanism (Del Carmen García et al., 2000;

Table 1
Physical and chemical properties crude oil samples.

Properties	Unit	Crude Oil Sample			Method
		A	B	C	
Appearance	–	Black	Brown	Black	Visual
Density at 15°C	kg/m^3	865	835	858	Measurement
Sp. Gravity	60°F/60°F	0.865	0.835	0.858	Calculated
API Gravity	–	32.1	35	33.4	API Method
Wax Content	wt%	11.5	19.7	15.3	Modified UOP 46-64
Wax Content	wt%	12.05	20.05	14[a]	HTGC (n-C15+)
Pour Point	°C	22	25.5	19.5	Rheometry
Pour Point	°C	23	26	20	Modified ASTM D-97
WAT at 120 1/s	°C	28.5	30	28	Rheometry
WAT at 10 1/s	°C	34	35	30	Rheometry
Viscosity at 45°C	Pa.s	0.0102	0.0056	0.0091	Rheometry
Viscosity at 15°C	Pa.s	2.31	3.89	1.20	Rheometry
Saturates Fraction	wt%	55.04	73.25	63.11	elution chromatography
Aromatics Fraction	wt%	34.67	21.2	31.01	elution chromatography
Resins Fraction	wt%	6.15	5.14	4.15	elution chromatography
Asphaltene Fraction	wt%	4.14	0.41	1.73	Modify ASTM D2007-80
CII	–	1.45	2.798	1.84	Calculated

Where the superscript "a" represented the wax content from correlation (see Equation (3.4)), Sample A, B and C are the Mwambe, KSG and synthetic crude oil.

Ragunathan et al., 2020). Crude oil with more than 50% saturate fractions is most likely to precipitate and deposit wax on the pipe wall. The deposited was can lead to unstable flow behaviour (Zhu et al., 2008; Moura et al., 2010). On the other hand, the aromatic components are acceptable solvents for asphaltene molecules in crude oil. They act as bridges between the mixed micelle and saturates and enable the mixed micelles to be effectively dispersed in saturates (Ashoori et al., 2017; Fan et al., 2002). This means aromatic fraction weakens the chains of asphaltene, which usually promote the interactions of waxes crystals and generally causes fouling (Chanda et al., 1998; Dickakian and Seay, 1988). The higher the aromatic fraction in the crude oil sample the more stable is the wax deposition. Whereas, a sample oil with high wax content would have a high saturated fraction with a low amount of aromatic fraction and vice-versa (Ekaputra et al., 2014).

Similarly, resin molecules in crude oil prevent any significant aggregation of the asphaltenes. As a result, the risk of asphaltene precipitation decreases as the resin content increases (Aske et al., 2002; Pereira et al., 2017). The study postulated that the resins assemble on the wax crystals and inhibit the interlocking process. Therefore, the stability of asphaltene in waxy oil would be improved by the presence of high resin and aromatic molecules.

2. Type of chemical wax inhibitors

The major types of chemical inhibitors used in the oil and gas industry include (i) wax crystal modifiers referred to as pour point depressants, (ii) Solvents, (iii) Dispersants, and (iv) Surfactants. The wax crystal modifiers have similar molecular structures to wax, and they are the most commercially used chemicals. If added to the crude oil, the modifiers co-precipitate with the wax crystals by replacing some of the wax molecules on the crystal lattices, hence, prevents wax molecules from networking and forming a lattice structure (Kang et al., 2014; Woo et al., 1984). Once adsorbed onto the paraffin crystal, they prevent agglomeration of the precipitated wax crystals. Examples of wax crystal modifiers include polyethylene, copolymer esters, ethylene/vinyl acetate copolymers, olefin/ester copolymers, ester/vinyl acetate copolymers, polyacrylates, polymethacrylates, and alkylphenol resins (Dobbs, 1999; Kang et al., 2014).

Solvents are used for the treatment of solid wax deposit and remediation formation damage. The added solvent in crude oil increases the solubility of wax in oil and dissolves already deposited wax (Kang et al., 2014). Dispersants are used to keep the pipe surface wet to minimise the tendency of the wax to adhere. These chemicals also help to disperse wax crystals into produce oil, thereby preventing the wax nuclei from agglomerating (Lee, 2008; Nguyen and Fogler, 2005). Nevertheless, the operational problem with this chemical is to maintain such a surface for an extended period. Surfactants are employed to clean pipelines and other parts of the system where wax may be deposited. Generally, the surfactants can promote the formation of a stable O/W emulsion, which is beneficial to pipeline transportation. They can be adsorbed onto pipe surfaces and decrease the adhesion of waxes to the surfaces possibly by changing the wettability of the pipe surface, creating an environment in which wax crystals are easily sheared off, adsorbing onto the wax crystals or preventing their sticking (Nguyen et al., 2001; Singh and Fogler, 1998).

In a nutshell, this study will improve the understanding of waxy oil behaviour through defined experimental methods. These methods are more refined and straightforward than those used by Zhao et al. (2015) and Paso et al. (2014). Hence, the aim of this study is to; (i) provide a comprehensive characterisation of different waxy crude oils, including analysis of SARA fractions, colloidal instability index, WAT, PP, wax content, n-paraffin fractions, and crystal morphology (ii) examine the performance of four commercial chemical inhibitors and (iii) investigate the synergistic effect resulted from blending different inhibitors. This works sheds light on new inhibitor development by blending different inhibitors to promote performance synergies.

3. Experimental methods – crude oil characterisation and wax inhibitors screening

Accurate oil properties are essential for the successful operations of the oil and gas industry. In this paper, a case-by-case investigation of crude oil assay blended with and without wax inhibitors was performed through several methods employed by standard laboratories and the oil industries. Essentially, inaccurate crude oil characterisation may lead to wrong designs of facilities and acts as bad input parameters for modelling and simulations. A programmable controlled shear rheometer rig, higher temperature gas chromatography (HTGC), Carl Zeiss Axiovert S100 inverted optical microscope equipped with a Motic digital camera and elution chromatography and other standard analytical techniques are utilized – including a modified acetone precipitation technique (UOP46-64), and ASTM D2549-02.

3.1. Model waxy oils

In most previous experimental studies, the complex rheology and other properties of different waxy oils are not thoroughly studied. At times, some of the studies use only a single crude oil sample or a synthetic sample. Their findings may be subjected to many limitations. When such data are applied to wax deposition modelling, the obtained results may be prone to severe uncertainty. Therefore, the experimental result of this paper could be used for validation of previous research trend for real crudes in order to maintain better control of the thermal history and also the composition, especially the gases. Three crude oil samples were studied. Two of the crude oil samples (KSG#49 and Ex Mwambe) subsequently referred to as sample A and B with unknown origins and properties were supplied by Roemex Oilfield Service Company, UK. Sample C was synthesized by blending solid wax supplied by Roemex with a dead crude oil provided by Core Laboratories Limited

Table 2
Chemistry of chemical inhibitors used in this study.

Inhibitors Code	Inhibitors Chemistry		
	Compositions	Percentage %	CAS
W2001	Hydrocarbons, C10, Aromatics, >1% Naphtalene (HAN)	30%–60%	n/a
	Olefinic polymer derivetive	30%–60%	1269781-05-6
W2003	Solvent naphtha (Petroleum), Heavy Aromatic	7%–13%	64742-94-5
	Distillates (Petroleum), Hydrotreated light	7%–13%	64742-47-8
	Naphtalene	1%–3%	91-20-3
W2004	Alkenes, C20 - 24 Alpha-, Polymers with maleic anhydride, C18-22 alkyl esters	60%–100%	n/a
	Solvent naphtha (Petroleum), Heavy Aromatic	7%–13%	64742-94-5
	Distillates (Petroleum), Hydrotreated light	7%–13%	64742-47-8
	Naphtalene	1%–3%	91-20-3
W2005	Solvent naphtha (Petroleum), Heavy Aromatic	7%–13%	64742-94-5
	Distillates (Petroleum), Hydrotreated light	7%–13%	64742-47-8

CAS (Chemical Abstracts Service) - a unique numerical identifier for chemicals.

Table 3
Blending of wax chemical inhibitors.

Inhibitors	Blended component
Blend A	50% W2001 + 50% W2003
Blend B	70% W2001 + 30% W2003
Blend C	50% W2001 + 50% W2005
Blend D	70% W2001 + 30% W2003
Blend E	50% W2001 + 50% W2004
Blend F	70% W2001 + 30% W2004
Blend G	50% W2003 + 50% W2004
Blend H	50% W2004 + 50% W2005

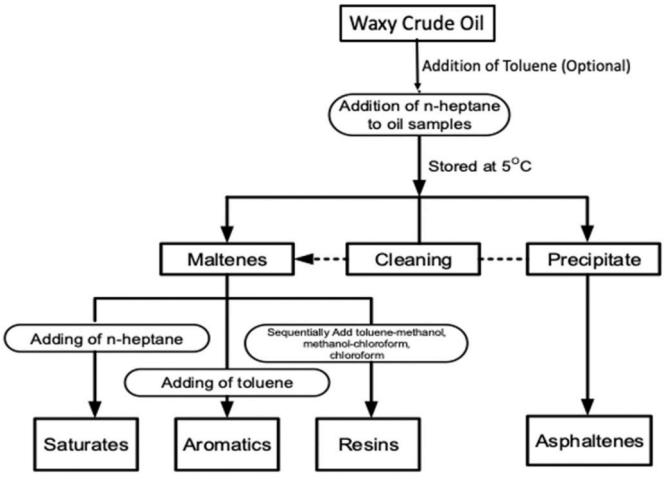

Fig. 2. Flow chart for crude oil sample fractionation (adapted from Zeng et al., 2012).

(UK). The dead oil has a shallow wax content (3 %wt) and a pour point of less than 1 °C. The primary rationale for synthesizing sample C is to form an oil with an increased wax content as it directly affects other properties such as the viscosity, pour point, and WAT (Bai and Zhang, 2013; Rehan et al., 2016). The wax content of synthetic crude was increased from 3 to 14 wt% according to the empirical formulations (Makwashi, 2020). In contrast, samples A and B are naturally waxy with wax content around 12 and 20 wt% (Table 1). According to Abdel-Waly (1997), a crude oil sample could be treated as Newtonian fluid if the wax content is relatively low (e.g. <5 wt% or even around 0.4 wt%).

3.2. Wax inhibitors/pour point depressants

Four chemical wax inhibitors (code: W2001, W2003, W2005, and W2004) were sourced from Roemex. However, the complete compositions of the inhibitors are not provided due to proprietary issues. Table 2 showed the chemical types and some of their compositions. The synergy of these four inhibitors was studied. 32 samples were tested, but only eight samples shown in Table 3 gave improved inhibition performance. The eight samples are mixtures with different component fractions, for instance, in blend B, D, and F, 70% of W2001 was blended with 30% of W2003, 30% of W2004, and 30% of W2005, respectively. And 50% of W2001 with 50% of W2003, W2004, or W2005 in blend A, C, and E. Chemical Inhibitor interaction is of great value in the area of flow assurance. A previous study by (Ruwoldt et al., 2019) investigates and evaluated the potential of new procedures for studying the interactions of different polymeric PPDs and asphaltenes in a waxy model system to extend the knowledge of wax inhibition. It is worth mentioning that in this work the criteria for blending different fractions of the inhibitors are based on the inhibitor's performance and their chemical composition.

3.3. Crude oil characteristics

A. API Gravity and Wax Content:

In the wax deposition experiment, crude oil characterisation is mandatory before the severity of the wax depositional problem can be evaluated in a flow loop. API gravity is one of the fundamental properties of crude oil that provides insight into oil quality. This property calculated using equation below. API gravity shows how heavy or light crude oil is compared to water.

$$API = \frac{141.5}{SG} - 131.5 \quad (1)$$

SG is the specific gravity (dimensionless quantity), defined as the ratio of the density of crude oil ρ_{oil} poil to the density of water ρ_{water}. In this work, a pycnometer was used to measure the density of the crude oil in reference to a well-known density of water (1 g/cm^3 or 1000 kg/m^3).

The wax content of oil samples is obtained by two different methods, (i) high-temperature gas chromatography (HTGC) (KAT Lab, 2009; Singh et al., 2011) and (ii) a modified UOP46-64 method known as acetone precipitation technique (Coto et al., 2011; Fan and Buckley, 2002; Hoffmann and Amundsen, 2010). The procedure of the HTGC method is detailed in the subsequent sections. In the modified UOP46-64 technique, 5 g of the oil sample is measured and mixed with 35 cm^3 of solvent (petroleum ether). The mixture is stirred in a beaker for about 15 min. Acetone is added to the mixture in a ratio of 3:1 vol/vol (acetone: petroleum ether) to precipitate the wax content in the oil. The mixture is then chilled to −20 °C for 24 h. The precipitate (i.e. waxes) is recovered by vacuum filtration using glass Buchner funnel with a vacuum pump connected to the filtration flask's sidearm. The filtered solid is washed with n-heptane to remove asphaltenes and the filtered liquid evaporated. Subsequently, the solid obtained after solvent evaporation is re-dissolved in n-hexane to remove asphaltene content and filtered again. After solvent removal, the final product (wax) was weighted, and the wax content (wt%) was determined.

$$\text{Wax content (wt\%)} = \frac{\text{weight of wax in crude (g)}}{\text{total weight of crude with wax (g)}} X\ 100 \quad (2)$$

B. SARA Analysis: Crude oil samples are separated into four petroleum fractions of Saturates/Aromatics/Resins/Asphalthene (Jewell et al., 1972) to assess crude's fouling propensity, blending compatibility,

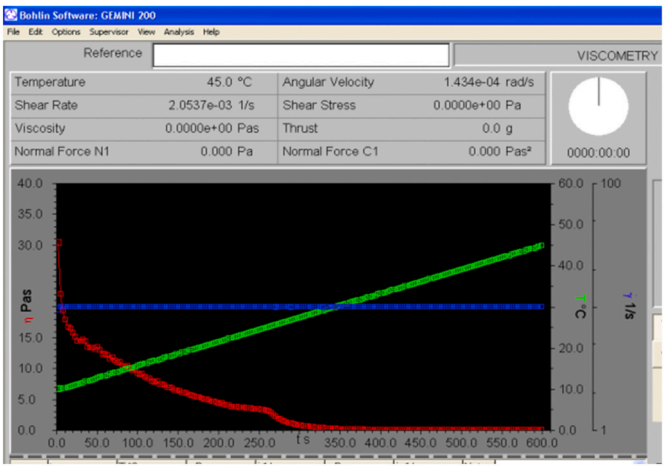

Fig. 3. A snapshot of viscometric data from Bohlin II rheometer at varied. Cooling temperature (50 – 0OC), constant shear rate (120/s).

and asphaltenic stability (Fan et al., 2002; Yen et al., 2001). Generally, SARA analysis provides an insight into the oil quality, oil-to-oil correlations, and is usually used to identify vertical and lateral oil quality gradients in reservoirs (Fan et al., 2002; Roenningsen et al., 1991; Wayne and Sue, 2015). Similarly, Zhu et al. (2008) reported SARA analysis is useful in assessing crude oil stability for wax related issues. In this study, a modified ASTM D2549-02 method (elution chromatography) was used to separate the fractions based on their polarities. The polarity of these fractions increases from low in saturates, to intermediate in aromatics, and high in resin. The step-by-step procedure is shown in Fig. 2. Asphaltenes fractions are the heaviest and most polar fractions formed by a series of relatively large molecules containing aromatic rings, several heteroaromatics such as nitrogen, sulfur, or oxygen atom, and naphthenic ring plus relatively short paraffinic branches (Deshannavar et al., 2010).

The crude oil was de-asphaltene before the open column chromatography separation of maltene. The de-asphaltene procedure adopted in this work is reported by Wang and Buckley (2002) (ASTM D2007-80 method) with a little modification from Ronningsen et al. (1991). Accordingly, 7 g of crude oil was mixed with 160 ml of n-heptane on a ratio 1:40 vol: vol (solvent to crude oil). The mixture was wrapped with aluminium foil and stored at 5 °C overnight. After aged overnight, the precipitated asphaltenes is recovered using Whatman® glass microfiber filters, Grade 934-AH®. The funnel cup is rinsed with precipitants before removing the filtered asphaltenes. Finally, the percentage of asphaltene weight fraction is calculated using Eq. (2) (Wang and Buckley, 2002).

On the other hand, 15 ml of maltene were charged into the chromatographic column using a pipette to recover saturate, aromatic, and resins after solvent removal from the produced maltene using vacuum evaporation. The sequential elution follows the study Jha et al. (2014). Initially, saturate fractions were eluted with 100 ml of n-pentane. While for the aromatics fractions, 100 ml of toluene were added, and the eluted aromatics are collected. The elution of polar resins was carried out in four runs. Each elution was collected separately, and the final products were added together. The elution procedure starts with mixing 100 ml of toluene-methanol solution at a volume ratio of 50:50, follows with 100 ml of methanol-chloroform solution at the same ratio, then uses only 100 ml of chloroform and ends with 100 ml of acetonitrile. All the eluted compounds were collected in different containers and separated from solvents using a rotary vacuum evaporator to recover the pure fraction of saturates aromatics and resins. The percentage of weight fraction was calculated.

C. Rheological Properties: The rheological study was performed using Bohlin Gemini II shear controlled Rheometer to measure the crude oil viscosity, wax appearance temperature (WAT), and pour point (PP). The same method is reported and used by Singh et al. (2011), Adeyanju and Oyekunle (2013), Perez et al. (2015), Wang et al. (2015), and Anton (2020).. In this study, the analysis was performed using a rotating cone with a 4^{O} angle, 40 mm diameter, and a gap specification of 0.15 mm (0150). Initially, the oil sample is heated above the wax crystallization temperature to eliminate the entire non-Newtonian characteristic. A pipette was used to introduce the sample oil on the stationary cylinder surface. The analysis begins by controlling oil temperature from 50 °C to 0 °C at a constant cooling rate of 1.0 °C/min and different shear rates (10, 60, and 120 1/s) similar to the study reported by Singh et al. (2011), Adeyanju and Oyekunle (2013),Theyab and Diaz (2016) and Wang et al. (2015). Once the oil sample reached 0 °C, the sample is held at that temperature for 15 min with no shear.

A complete experimental run captured on a PC is shown in Fig. 3. The measured viscosity is represented by a Red-line at different cooling temperature (Green line) and constant shear rate (Blue line). Wax appearance temperature (Cloud point temperature) of the sample is usually characterised by any deviation point from the horizontal line of the viscosity line as shown below, otherwise, as an intersection of a baseline drawn from the Newtonian region and a tangent that fitted to the inflexion point (see Section 3D). Whereas, the point of inflexion after the WAT point is defined as the pour point.

Similarly, the oil is doped with wax inhibitors – different inhibitor was screened by measuring the efficacy to reduce viscosity and delay WAT and PP at three different concentrations (500, 1000 and 1500-ppm) with a constant shear rate (120 1/s) and cooling rate (°C/min).

D. Pour Point Analysis: A slightly modify ASTM D-97 method is employed. The technique has been the easiest and quickest method for measuring the pour point of waxy crude oil (Alcazar-Vara and Buenrostro-Gonzalez, 2011; Coto et al., 2014; Roenningsen et al., 1991). The results are compared and validated with viscometric plot analysis (Adeyanju and Oyekunle, 2013; Theyab and Diaz, 2016a) described in the subsequent paragraph. The modified ASTM D97-08 standard procedure started by preheating an appropriate amount of crude oil in a test jar to about 60 °C for 5 min. The complete set-up is made of a bath with crushed ice. The test jar sealed with a cork is placed in the bath. A thermometer is partially immersed in the sample through the sealed cork to monitor the temperature changes. The pour point was observed and checked after every minute. The test jar is removed and positioned horizontally if the crude oil remained in that position for 5 s without sagging. The temperature reading is recorded. According to ASTM D-97, the actual pour point is 3 °C higher than the reading observed. So 3 °C is added to the thermometer reading as the PP of the sample.

E. Crystal Morphology of Wax in Crude Oil: A Carl Zeiss Axiovert S100 inverted optical microscope equipped with a Motic digital camera was used to study the crystalline wax molecules' microscopic morphology in crude oil samples. Through this study, the strong interlocking and interactions of the wax crystals, which formed a gelled network (Coto et al., 2014; Yang et al., 2014) in the pipeline are evaluated. On the other hand, the effectiveness of chemical wax inhibitor on the paraffin crystal structures was observed and analysed. The inhibitor's presence is expected to affect the structural formation of the wax crystals and agglomeration of particles. Overall, the analysis was conducted with oil samples doped and undoped chemical inhibitor at 1000-ppm, and 15°*C*.

F. Colloidal Instability Index (CII): CII is used as a screening criterion for the tendency of soluble asphaltene in crude and the extent of its problem (Ashoori et al., 2017; Yen et al., 2001). Therefore, CII was used in this work to scale the propensity of asphaltene aggregation of the crude oil samples. CII considers crude oil as colloidal systems consisting of pseudo components of saturates-aromatics-resins-asphaltenes and is expressed as the ratio of the sum of asphaltenes and their flocculants (saturates) to the sum of their peptisers (aromatics and resins) in crude oil (see Eq. (3)).

Table 4
C10-60 standard Volume.

Concentration (mg/ml)	Carbon Number	RT (mins)	Area (pA*s)	Sensitivty (pA*s/ng)
0.058	10	3.02	477.56	16.467
0.048	20	14.01	497.79	20.741
0.048	30	21.49	547.01	22.792
0.050	40	26.91	541.40	21.656
0.050	50	31.11	530.93	21.452
0.050	60	34.51	433.62	17.345

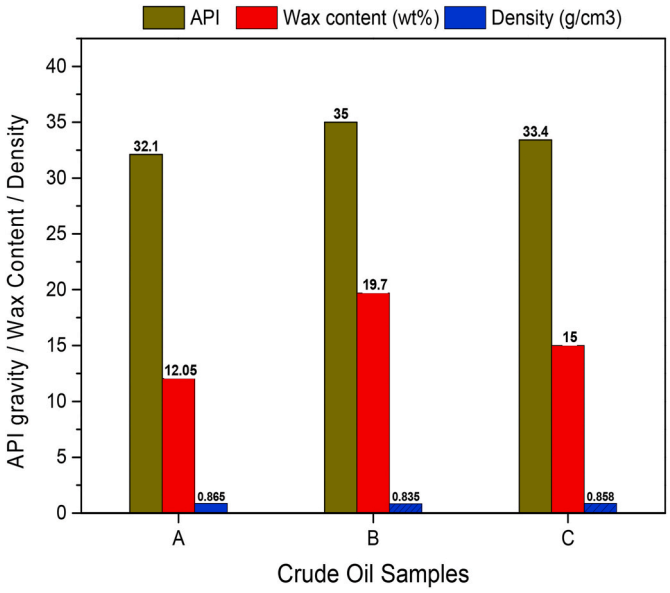

Fig. 4. API, density, and wax content of three crude oil samples.

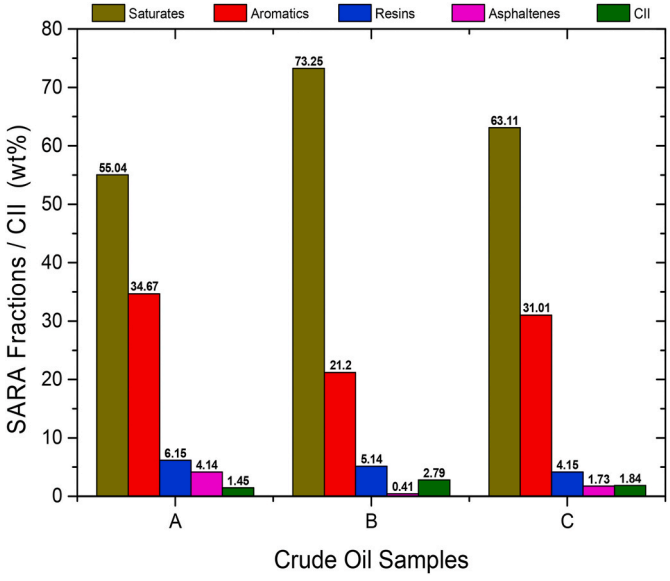

Fig. 5. SARA fraction of crude oil samples and colloidal instability index (CII).

$$CII = \frac{\text{Saturates} + \text{Asphaltenes}}{\text{Aromatics} + \text{Resins}} \quad (3)$$

According to Asomaning and Watkinson (2000) and Yen et al. (2001), if the oil CII value is above 0.9, the oil has a propensity to asphaltene aggregation, which is regarded as very unstable oil. If the CII is lower than 0.7, the oil has a solubilise asphaltene. Hence, oil is stable. However, if the CII falls between 0.7 and 0.9, the oil has moderate instability.

G. n-Paraffin Distribution: Higher temperature gas chromatography (HTGC) was used to study the distribution of n-paraffin and wax content of the crude oil (Coto et al., 2011; Singh et al., 2011; Zheng et al., 2016). This analysis was carried out in collaboration with the University of Plymouth using a commercial technique known as T-SEP® – thermal separation technique, which was co-developed by the University of Plymouth and Kernow Instrument Technology UK. The technique is currently one of the most reliable, reproducible and effective methods compared to some of the conventional techniques employed by most laboratories (KAT Lab, 2009). According to KAT, the method allows precise control of hydrocarbon by "*topping process*". On average, the methods allows an additional 20 carbon numbers of the n-paraffin to be observed and measured. It is worth noting that only two samples (A and B) were analysed using this novel method due to the cost involved.

The set-up consists of an Agilent 6890 gas chromatograph equipped with flame ionization detector (FID) and a Varian Vf–5ht Ultimetal column (15 m × 0.25 mm x 0.1 μm). The oven is programmed to run from 40 to 435 °*C*at 10 °*C*/min ramps before holding at 435°*C* for 10 min. Helium was used as carrier gas at 5 ml/min. Initially, the crude oil was heated at 70 °C for 1 h, and a small amount of heated oil was dispensed using foil-wrapped glass in two pre-weighed containers that were pre-heated at 110 °C. The containers were then sealed and kept at room temperature. The two samples prepared from each oil were analysed and referred to as the ***Whole Sample*** – this is unadulterated crude oil and is made up to the required concentration of 5 mg ml^{-1} with cyclohexane as a solvent and then analysed with HTGC at 0.5 μL. ***Topped Sample*** is prepared according to the novel T-SEP® technique with *undisclosed solvent* in this work subject to various confidentiality agreements.

It is worth noting that during the standard analysis of whole oil sample as reported by KAT Lab (2009), the concentration of nC_{10}–C_{20} is relatively higher than the n-paraffin > nC_{20}^{+} fractions. Perhaps this is because the n-paraffin > nC_{20}^{+} is slightly closer or below the limit of the HTGC instrument detection – especially for crude oil with a broader range of carbon (>nC_{50}^{+}). This implies that the heavier n-alkanes reported by this procedure may not have sufficient accuracy and do not represent the full range of carbon in that particular sample. This topping procedure can resolve this problem. By this method, the concentration > nC_{15}^{+} are accurately measured and all the n-alkanes < nC_{15} and unresolved complex mixture are eliminated or reduced. The peaks of n-Paraffin of samples are quantified relative to the chromatograms of solvent blank (cyclohexane), the compound in C_{10}–C_{60} standard (Table 4) and Polywax 655 external standard. The response factors interpolated between C_{10}–C_{60} and carbon numbers > nC60 are quantified using the response factor of nC60. Whereas, the retention times are correlated with Polywax 655 external standard as discussed in the results section.

Unlike the conventional methods that produce the peak areas' ratio to the total chromatogram signal area, T-SEP® technique converts the integrated peak area to a mass (ng) of a relevant external standard. The converted mass is represented as a weight percentage relative to the injected oil's mass (typically 10 μg). Details of these were reported in KAT Lab (2009) and Makwashi et al. (2019). As stated by KAT Lab (2009), the rationale for this approach is that "the entire chromatographic area represents only the GC amenable part of the oil. So injecting the same mass of different oils will produce different total chromatogram areas, depending upon how much of each of the oils is GC amenable". Similarly, if 10-ppm of C15 is injected the peak area will not be the same as if 10-ppm of C60 is used (KAT Lab, 2009).

4. Results and discussion

A. API Gravity and Wax Content of Oil Samples

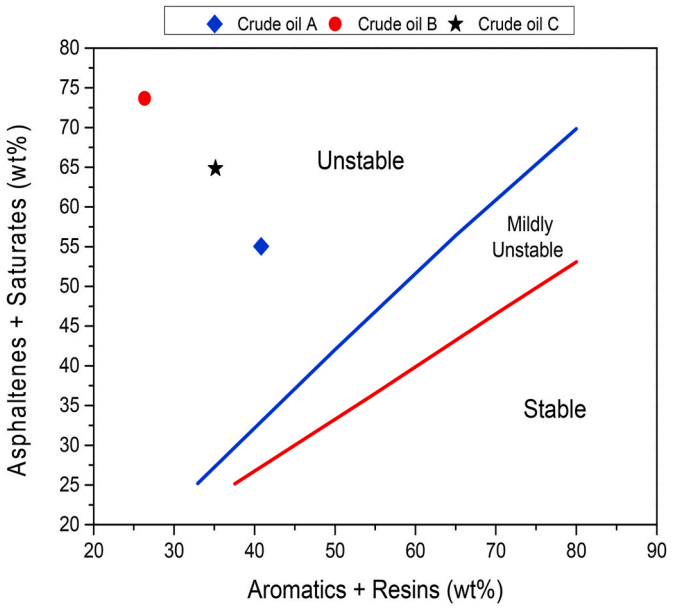

Fig. 6. Analysis of crude oil samples instability using Yen's mode.

Typically, crude oil samples are classified according to their gravities, which could be either heavy or light crudes. Therefore, light crude oils are usually regarded as less dense with high API gravities (>33°API). Typical light crudes usually have high paraffinic content and high amount of dissolved gases. Whereas, the denser crude oil are those with low API gravity (<28°API), consisting of more asphaltenes, higher aromatic/naphthenic contents, and a small fraction of dissolved gases (American Petroleum Institute, 2011; Sifferman, 1979). Hence, in this work, the API gravities of samples A, B, and C are 32.1, 35, and 33.4 API, respectively (Fig. 4). As expected, sample A with a density of 865 kg/m^3 is relatively denser than samples B (835 kg/m^3) and C (858 kg/m^3).

Similarly, the wax content as an indicative parameter of the sample's depositional tendency is shown in Fig. 4. It is found that the modified UOP 46–64 and HTGC methods give similar wax content results (Table 1). Sample B has the highest wax content of 19.7 wt% by UOP 46–64 method and 20.05 wt% by HTGC. While Sample A has wax content of 11.5 wt% (UOP 46–64) and 12.05 wt% (HTGC) and Sample C has 15.3 wt% (UOP 46–64) and 14 wt% (HTGC) respectively. Therefore, based on these values all the samples are characterized as highly waxy crudes. Some previous study (such as Holder and Winkler, 1965; Kasumu, 2014; Sarica and Panacharoensawad, 2012) have shown that a crude oil containing as little as 2% by mass of wax can potentially cause deposition problems, particularly under suitable conditions that favour the process.

B. SARA Fractions and Colloidal Instability Index.

Fig. 5 shows the SARA fractions and colloidal instability index (CII) of model oils (A, B, and C). It is observed that the saturates fractions in sample B is higher (73 wt%) than those in sample A and C (55.04 and 63.22 wt%). However, the three samples have sufficient fractions of saturates, which defined the samples as highly paraffinic (Ekaputra

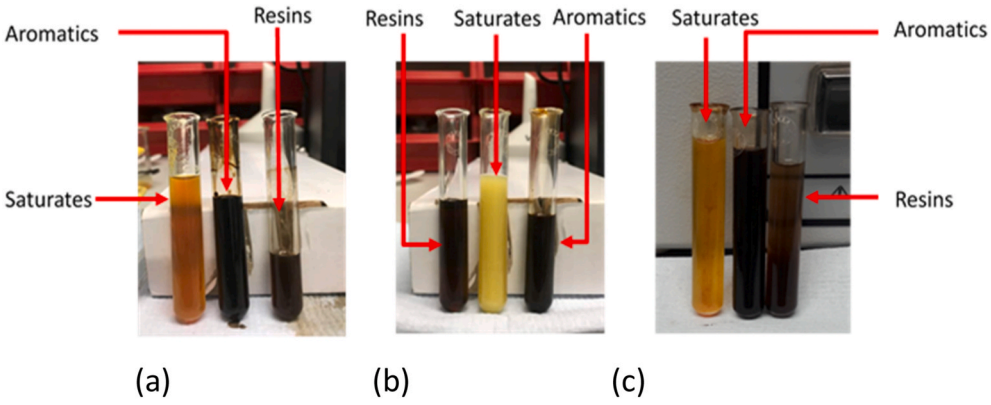

Fig. 7. Sample fractions of Saturates, Aromatics and Resins: (a) crude oil sample A, (b) crude oil sample B and (c) crude oil sample C.

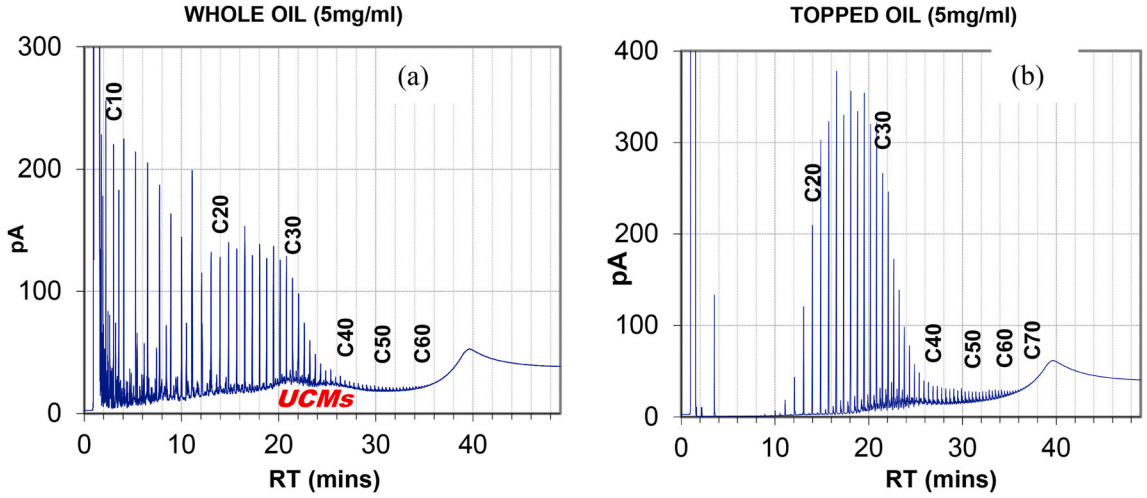

Fig. 8. Chromatogram of sample A crude oil. (a) Whole oil chromatogram. (b) Topped oil chromatogram.

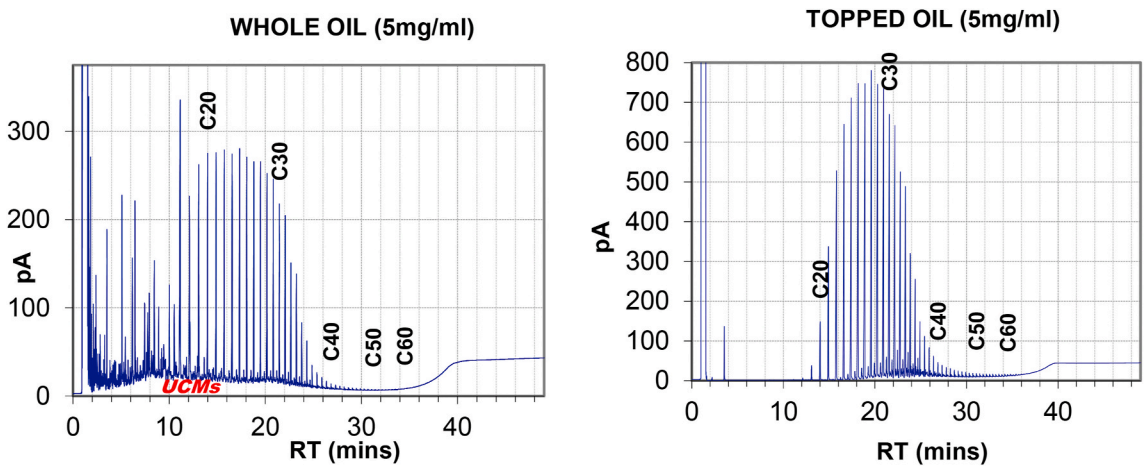

Fig. 9. Chromatogram of sample B crude oil. (a) Whole oil chromatogram. (b) Topped oil chromatogram.

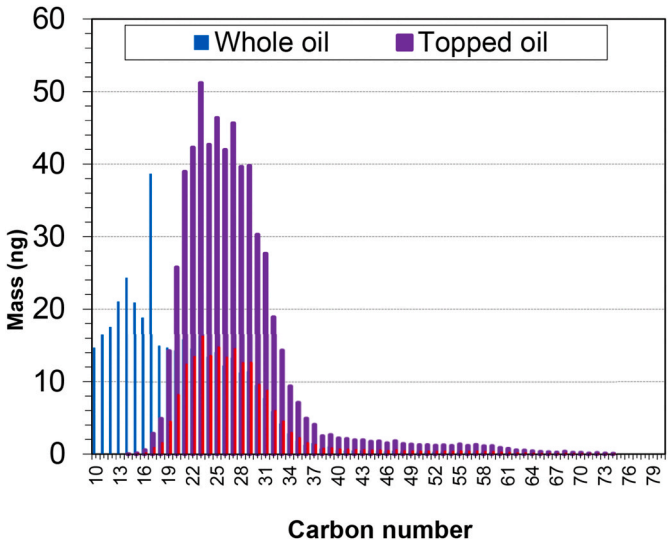

Fig. 10. Correlation chart for waxy crude oil sample A.

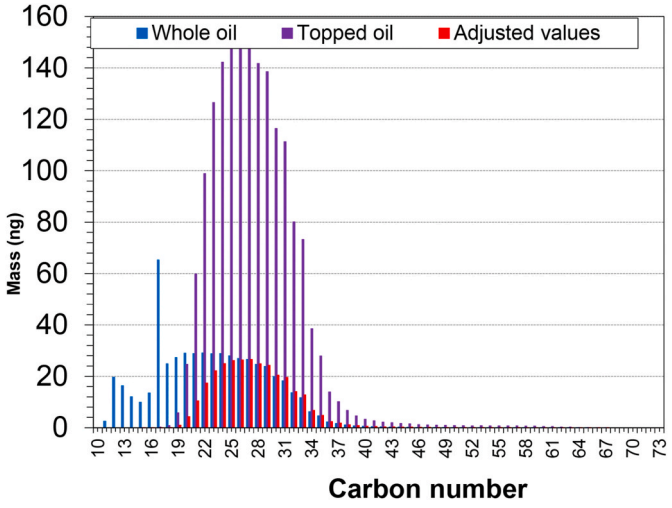

Fig. 11. Correlation chart for waxy crude oil sample B.

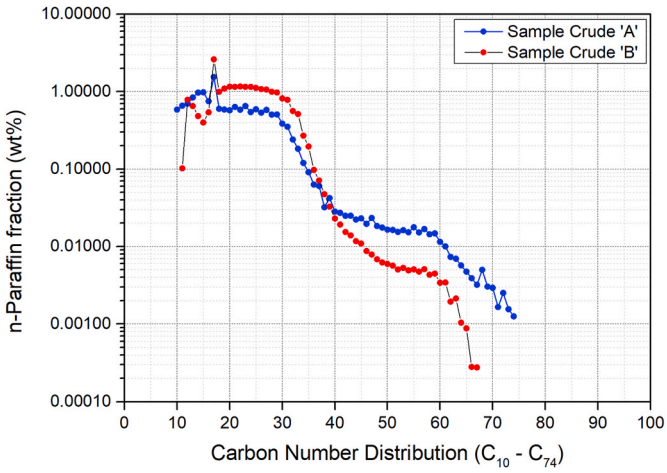

Fig. 12. n-Paraffin distribution of waxy crude oil samples A and B.

et al., 2014). Studies have shown that crude oil with more than 50% saturates (flocculants) is most likely to precipitate and deposit wax – leads to highly unstable flow behaviour (Moura et al., 2010; Zhu et al. 2008). On the other hand, the aromatic components are higher (34.67% wt) in sample A than in B and C (21.2 and 31.01%wt). This means that the presence of a high aromatic component (e.g., sample A) could retard the gel structuring process of higher asphaltene fraction (4.14 wt% in A) via steric interference (Paso, 2014) and result in a significantly weaker gel structure. It is expected that oil sample with a higher aromatic component to be more stable with respect to wax deposition – therefore has less wax content. In other words, a sample oil with high wax content would have a high saturated fraction with a low amount of aromatic fraction and vice-versa (Ekaputra et al., 2014). However, as seen in Fig. 5, the low amount of resin fraction in samples A, B, and C (6.15, 5.14, and 4.15 wt%) suggests the samples' instability. This is due to resins as natural gelling point depressants. A sufficiently high content of resins in crude oil could potentially prevent any significant aggregation of the asphaltenes.

The samples' instability was further evaluated using Yen's model (Ashoori et al., 2017). Fig. 6 demonstrates that all the model oil samples are unstable. This is because the CII of the samples' calculated (using Eq. (3)) are greater than 0.9. The CII of samples A, B, and C are 1.45, 2.79, and 1.84, respectively. Sample A with higher asphaltene fraction (4.14 wt%) and higher resin value (6.15 wt%) has a relatively lower CII value of 1.45, compared to 2.79, and 1.84 for sample B and C, respectively. This implies the instability increases from the low fractions of aromatics

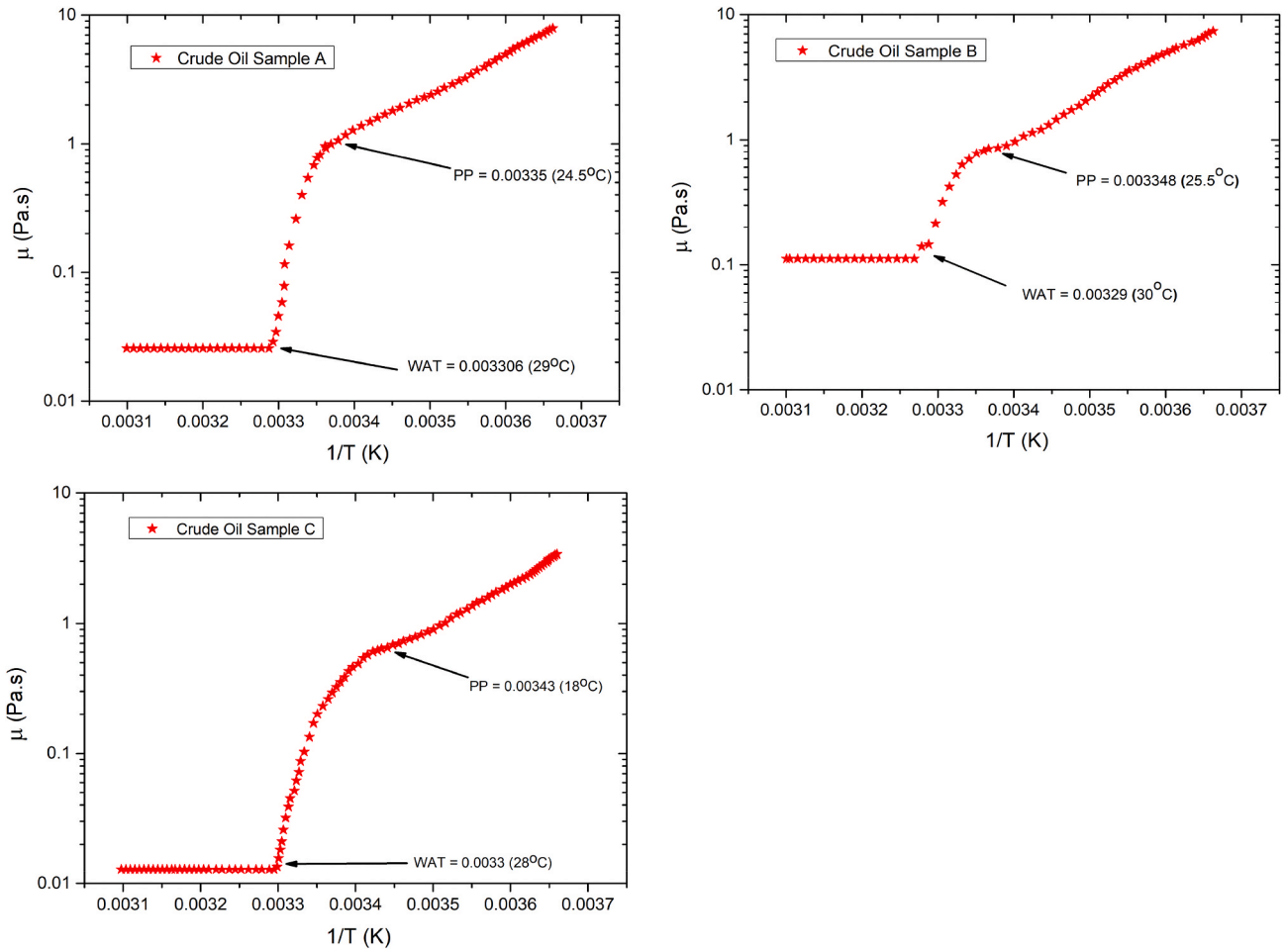

Fig. 13. Influence of varied Temperature at constant Shear Rate (120 1/s) on WAT, PP and Viscosity of (a) samples A crude (b) sample B and (c) sample C crude oil.

and resins to a higher saturate and asphaltene, as suggested by Ashoori et al. (2017).

Similarly, the crude oil and its fractions could be distinguished by their colours. The visual inspection of the actual crude oil samples shows that Samples A and C appeared as black, perhaps due to the amount of asphaltene fraction, whereas, sample B is brown. The results of SARA fractions (Fig. 7) showed that the saturated fraction in sample A and C are pale yellow, while sample B, on the other hand, is more pure yellow. The aromatic fractions are found as a dark brown liquid, while the resin fraction is Gardner or clear light brown liquid. In general, the colours depicted in this figure agreed with those reported by Benedek (2000) and Odebunmi et al. (2002).

C.n-Paraffin Distribution of Crude Oil Sample

The analysis of n-Paraffin allows the carbon to be categorised into macro-crystalline (C_{15} – C_{36}) and micro-crystalline (C_{36} – C_{60}^{+}) using HTGC. Through this analysis, the wax content of crude is estimated and validated with the modified UOP46-64 method. The analysis procedure was set as follows: Firstly, the chromatographs of solvent blank (cyclohexane), the compound in C10-60 standard, and Polywax 655 external standard were determined (Makwashi, 2020). Subsequently, the complete oil analysis resulted in a series of chromatograms containing unresolved complex mixtures (UCMs), as shown in Fig. 8 and Fig. 9. These unresolved complex mixtures (UCMs) are often found during the normal HTGC analysis (Hasinger et al., 2012; KAT Lab, 2009) and generally affect the results' accuracy. In reality, the whole oil chromatographs did not reflect the actual n-paraffin distribution within the oil samples, and therefore, the n-paraffins content is underestimated (Fig. 8 a). Hence, in these chromatograms, the n-paraffins fractions above $C30^{+}$ are considered to be below the detection limit of HTGC (KAT Lab, 2009). In both A and B, the peak intensity was observed to decrease sequentially from n-Decane C_{10} – C_{60}.

However, as shown in Fig. 8 (b), the topping procedure allows the heavier compounds to be detected with higher precision (KAT Lab, 2009). Also, the fractions of the unresolved component mixture (UCM) are minimised to a great extent. Therefore, the n-Paraffin fractions' peaks, particularly C_{15}–C_{35} (macro-crystalline) become highly intensified, while those above C_{30}^{+} are more pronounced, and the UCM are resolved. Higher peak intensity was found in sample B around the macro-crystalline molecules, compared to sample A. This implies a higher amount of wax content in sample B. Whereas, the larger peaks of the ' distributed carbon between (C_{40} – C_{74}) in sample A (Fig. 8) could be attributed to the higher asphaltene content in the sample.

Based on the T-SEP® procedure (KAT Lab, 2009), the data of 'whole' and 'topped' oil were merged to produce a new "an adjustable value" (Figs. 10 and 11), which represents the actual n-paraffin distribution in the crude oil samples (Fig. 12). It is found that Sample A has a carbon distribution between C_{15} – C_{74}, whereas C_{15} – C_{67} for sample B crude oil. Data merging was carried out via a mathematical correlation developed as part of T-SEP® technique. It clearly demonstrates the differences between the macro and microcrystalline waxes as a result of different functional properties (including viscosity and melting point) due to their varied hydrocarbon contents (França et al., 2018).

Fig. 12 shows that the distribution of n-paraffin of the two samples around macro-crystalline fraction increases from C_{15} to around C_{27} and then gradually decreases towards the C_{36} and toward the higher molecular weight component of microcrystalline wax. The macro-

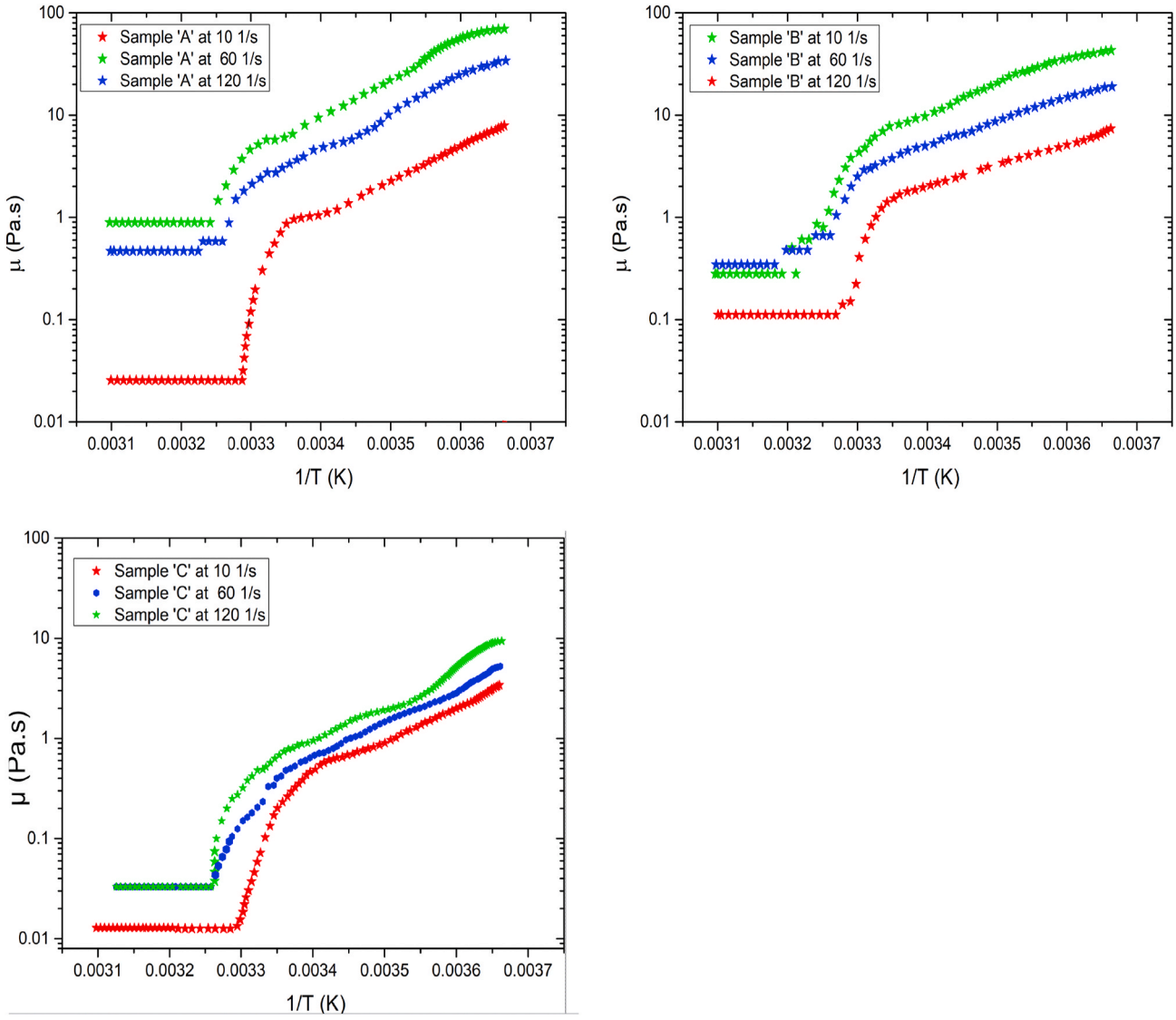

Fig. 14. Influence of different shear rate (10, 60, 120 1/s) on viscosity, PP and WAT: (a) Sample A crude oil, (b) Sample B and (c) Sample C.

crystalline wax components in sample B ($C_{15} - C_{36}$) varies from 0.196 to 1.161 wt%, whereas the micro-crystalline fraction from 0.0003 to 0.097. On the other hand, the macro-crystalline wax of sample A ($C_{15} - C_{36}$) varies from 0.092 to 0.835 wt% and the micro-crystalline wax molecules from 0.001 to 0.063 w%. This indicates a higher fraction of microcrystalline wax crystals in sample A than that in Sample B. This could be as a result of the higher amount of asphaltene in sample A. Whereas, a higher fraction of macrocrystalline in sample B than in A could be related to the higher saturate fraction of sample B.

A unique peak was seen at C_{17}, which corresponds to the n-paraffin fraction of 2.31 wt% for sample A and 1.546 wt% for sample B. This behaviour discussed in Makwashi (2020) could be due to the colluding of some Pristane ($C_{19}H_{40}$) fractions with nC_{17} as they have approximately the same boiling points. The inability to distinguish these two compounds by T-Sep technique is pointed out as the limitation of this novel method (KAT Lab, 2009). However, it is understood that this behaviour does not affect the accuracy of the results.

D.Analysis of Crude Oil Rheological Properties and Chemical Wax Inhibitors

Wax crystals are soluble in crude oil particularly at reservoir condition (70 -150^{O}C). As the temperature begin to drops, wax-oil gel systems are formed that possess mildly shear-thinning and exhibit strong rheomalaxis behaviour (Rodriguez-Fabia et al., 2019). Following crude oil properties determined in Fig. 13, wax inhibitors are also screened, and the synergy of different inhibitors was further studied to improve the inhibition performance by reducing viscosity, pour point, and WAT. Among the four original samples, W2001 produced the best inhibition performance to reduce viscosity and delayed WAT and pour point. Similarly, a new blended sample (A) displayed an improved performance compared to other tested chemicals.

i. Effect of Temperature and Shear Rate on the Crude Oil Properties

Crude oil properties such as pour point and wax appearance temperature (WAT) were measured instantaneously as the wax crystal precipitated during the shear controlled analysis. Fig. 13 showed that as the concentration of wax particles along the pipe is appropriately high due to the drop in temperature, the fluid flow gradually changes from Newtonian to non-Newtonian behaviour. This implies that the crude oils exhibit non-Newtonian behaviour as the temperature continues to drops close to its pour point. As shown in Fig. 13 WAT represented the beginning of wax crystallization (Adeyanju et al., 2013; Alcazar-Vara and Buenrostro-Gonzalez, 2011; Anton Paar, 2020; Huang et al., 2015; Perez et al., 2015; Roenningsen et al., 1991; Ruwoldt et al., 2018; Singh et al., 2011; Theyab and Diaz, 2016b),. According to section 3.3C, WAT represents any deviation point from the Newtonian region, which is

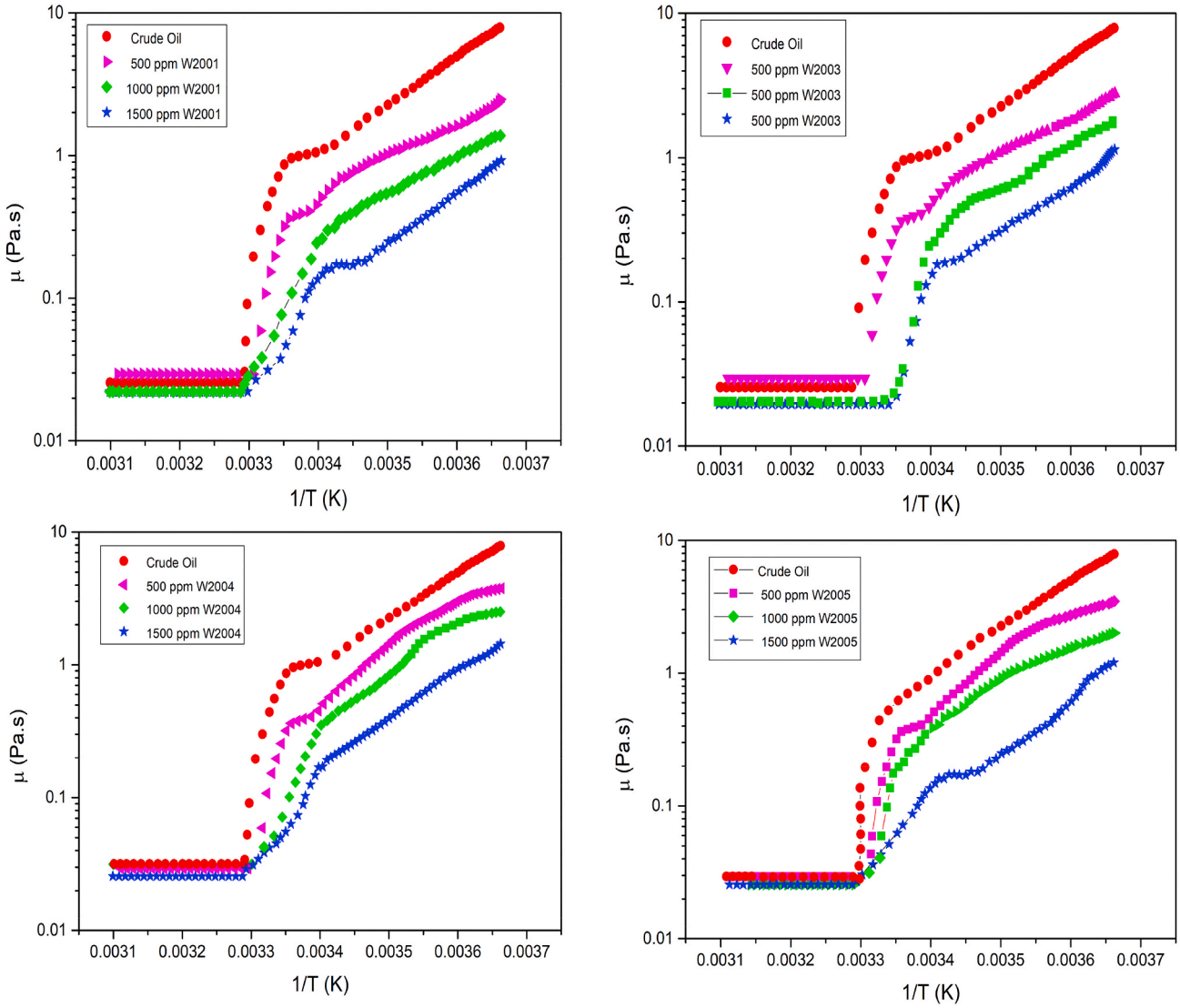

Fig. 15. Rheological behaviour of sample B crude mixed with different inhibitor at a constant shear rate of 120 1/s and varied temperature and concentration: (a) W2001, (b) W2003, (c) W2004 and (d) W2005 inhibitor.

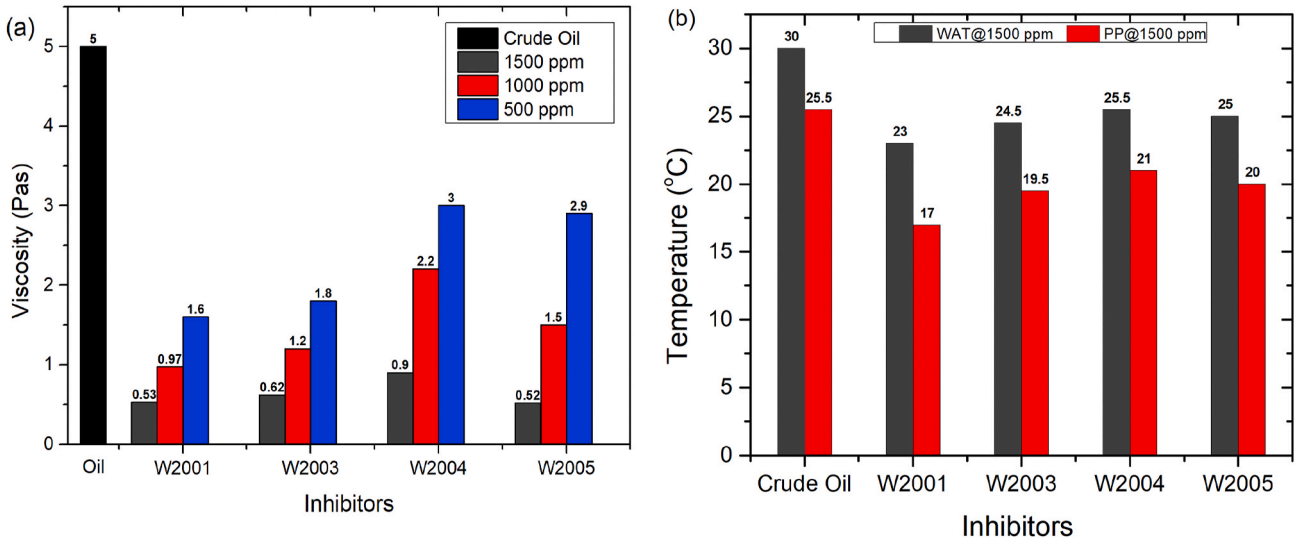

Fig. 16. Effect of chemical inhibitors on (a) viscosity at 5 °C and shear rate of 120 1/s and (b) pour point at a shear rate of 120 1/s at varied cooling temperature (0–50 °C).

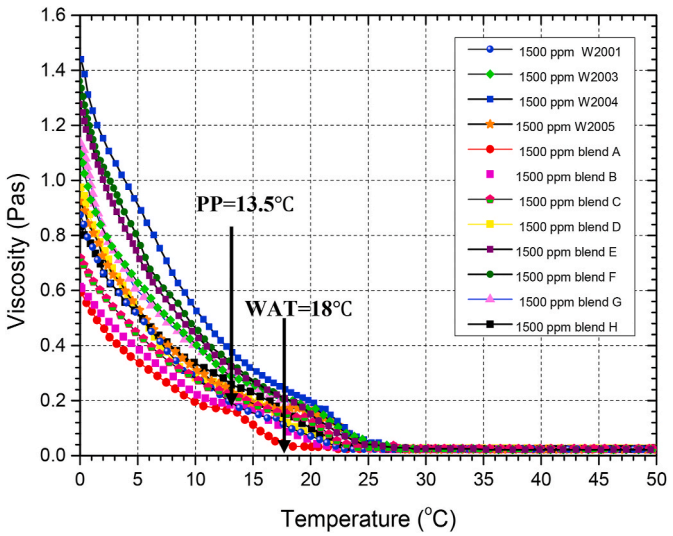

Fig. 17. Performance of different inhibitors on the rheological behaviour of oil at constant concentration (1500 ppm) and shear rate (120 1/s).

approximated by a point of intersection of two straight lines as shown in Fig. 13. In contrast, the pour point is defined as the intersection point between two tangent lines drawn from the inflexion point after the WAT. The pour point obtained from this method was validated by modifying the ASTM D-97 method.

It is observed that sample B crude with higher wax content displays the highest pour point (25.5°*C*) and WAT (30°*C*) (Fig. 13b). Therefore, to avoid the deposition problem, it is desirable to maintain the flowline temperature above 30°*C*. As the temperature drops, the propensity of the samples to crystallise and form solid wax is higher. On the other hand, a possible re-start problem is observed in the oil samples due to the high pour point, which is generally related to high paraffin content (Bai and Zhang, 2013; Ekaputra et al., 2014; Zheng et al., 2017). As expected, the more viscous the oil sample, the higher the wax content. However, sample A was found as a highly viscous fluid, for instance, 2.1 Pa s at 15°*C* and 0.03 Pa s at 50°*C*, compared to sample B and C, perhaps due to its high asphaltene content.

The influence of different shear rates (10, 60, and 120 1/s) at varying temperatures (0–50°*C*) on WAT, PP, and viscosity of the samples is shown in Fig. 14. As observed, the oil viscosity varies inversely with shear rate and temperature. Hence, as the shear rate reduces with a decrease in crude oil temperature, the pseudoplastic behaviour begins to appear; therefore, the crude oil properties change with shear rate. Otherwise, the crudes typically behave as Newtonian fluid above the pour point. This behaviour demonstrates that shear and oil temperature are particularly crucial within which flow assurance strategies are designed. The oil viscosity increases as a result of the precipitated crystals in the bulk fluid (Fig. 14). The rate at which the precipitation occurs is dependent upon thermal history, temperature, shear rate, and wax composition. Therefore, at a higher shear rate the cohesive and the adhesive force between the wax molecules and the deposition surfaces are overcome. For example, at a low shear rate of 10 1/s, high viscosity and relatively high WAT values are seen in the three crude oil samples. At 10 1/s and 10 °*C*, sample 'A' crude oil viscosity is 30 Pa s, which reduces to 15 and 5 Pa s at 60 and 120 1/s. Similarly, WAT of sample A increases from 28.5°*C* to 35°*C*as the shear rate drops from 120 to 10 1/s. Sample B and C displays similar behaviour. Hence, WAT increases from 30 to 36°*C* and from 28 to 33°*C* when the shear rate drops from 120 to 10 1/s, respectively. Perez et al. (2015) and Theyab and Diaz (2016a) reported similar crude oil behaviour.

ii.Effect of Wax Inhibitors on Crude Oil Rheological Properties

Four commercial inhibitors at different concentrations were investigated on the rheological properties of Crude oil B. Sample B crude is chosen because of its propensity to cause more problems than the other samples, as indicated by wax content, API gravity, n-paraffin, PP, and WAT. The shear rate was set at 120 1/s and the inhibitor concentrations were chosen at 0-ppm (zero inhibitors), 500-ppm, 1000-ppm, and 1500-ppm. The oil temperatures range from 0 to 50°*C*. The shear experienced by flowing fluid in an oil pipeline is higher than those experimented in the Lab. Therefore, 120 1/s chosen in this section is more appropriate than the lower shear rates. Similarly, this shear yields approximately the same pour point as the modified ASTM D-97 method. It is observed in Fig. 15 that all the four inhibitors have effectively decreased the oil viscosity, thereby reduce wax appearance temperature and pour point of the crude. These suggested that the chemicals must have interfered with nucleation, growth, and agglomeration of the wax crystals. These inhibitors are Polymer-based with similar structures to the wax crystals, hence, they easily incorporate themselves into the active sites of the wax crystals and thereby prevent the crystals growth and promote the formation of smaller aggregate particles (Adeyanju and Oyekunle, 2014; Jennings and Newberry, 2008).

The performance of the inhibitors reduces as the concentration decreases. Hence, wax inhibitor W2001 provides the best inhibition performance – by reducing WAT, viscosity, and PP. At 1500 ppm, the WAT and PP of oil blended with W2001 reduces from 30 to 24.5°*C* and 25.5 to 19°*C*, respectively (Fig. 15). Whereas the viscosity at 5°*C* was reduced from 5 Pas (undoped) to 0.25 Pas. Overall, the inhibitor's performance decreases in the order of W2001 > W2003 > W2005 > W2004. This implies that, apart from the concentration, the performance is influenced by the inhibitors' composition. Similar behaviour was reported by Erceg Kuzmić et al. (2008), Hoffmann and Amundsen (2013), and Pedersen and Rønningsen (2003). As stated early in this paper, the complete composition of these commercial inhibitors was not provided by the company, however, based on the available data, the effectiveness of inhibitor W2001 can be attributed to its better compositions that can promote smaller aggregate formation than the others. W2001 is made-up of a mixture of Olefinic polymer derivatives – regarded as a very good pour point depressant. Other compositions included hydrocarbons C10, Aromatics, and Naphthalene in different percentages.

W2003, the second-best inhibitor, consists of solvent naphtha, heavy Aromatic, distillates (petroleum), hydrotreated light Naphthalene, Alkenes: C20 - 24, Alpha-Polymers with maleic anhydride, and C18-22 alkyl esters. However, very little inhibition difference was observed between W2003 and W2005 inhibitors, particularly at 1000 and 1500 ppm. Because the two inhibitors have similar compositions except that Naphthalene was found in W2003. Inhibitor W2004 displayed the most deficient performance amongst the tested samples.

It is observed that during the controlled cooling at 5 °C and at a lower concentration of 500 ppm the viscosity of undoped sample (pure crude oil) reduces from 5 Pa s to 2.9 Pa s and 2.60 Pa s for W2004 and W2005 inhibitors. This reduced further to 1.75 and 1.6 Pa s with W2001 and W2003 inhibitors at the same condition above (Fig. 16, a). The pour point and WAT of crude oil give further evidence of the effectiveness of inhibitor W2001 compared to others (Fig. 16, b). It is observed that for W2001 inhibitor at 500, 1000, and 1500 ppm, the pour point of crude oil sample decreases from 25.5°*C* (pure crude oil) to 22°*C*, 20.5, and 17°*C* while the wax appearance temperature decreases from 30°*C* (pure crude) to 29, 25.4, and 23°*C* respectively. These suggested that at a low concentration, there are no sufficient chemicals to prevent wax formation effectively. Therefore, increasing inhibitor concentration leads to a decrease in the pour point and wax appearance temperature. Overall, it is well comprehended that in addition to the flow conditions (e.g. shear rate, shear stress, and temperature), the concentration and composition of chemical inhibitors influence crude oil's rheological properties.

iii.Performance of Blended Wax Inhibitor on Oil Rheological properties

As inhibitor composition significantly impacts its performance, blending two or more inhibitors could generate a synergy effect. Fig. 17 presents the viscometric analysis of crude oil (sample B) doped with

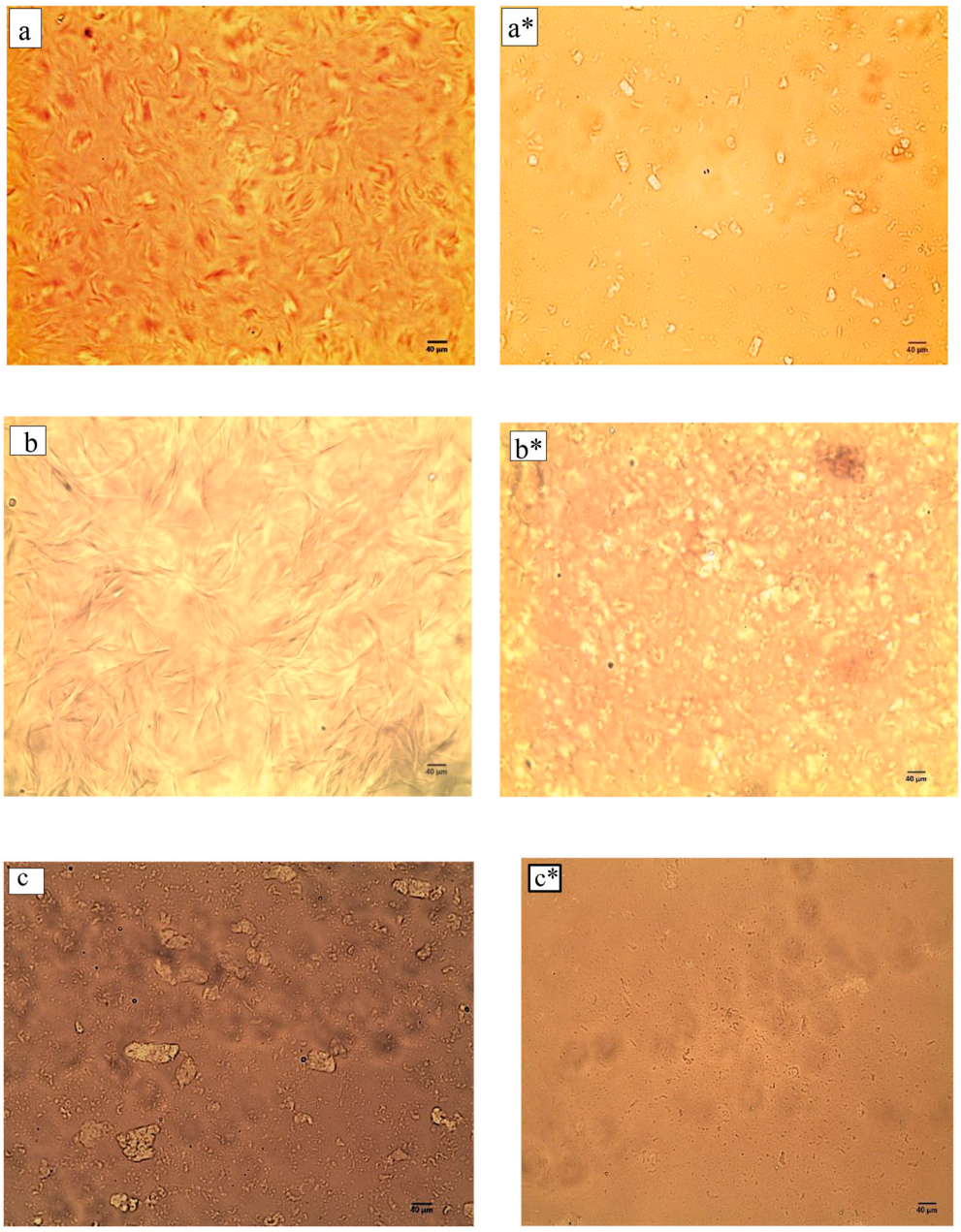

Fig. 18. Photomicrographs of crude oil samples a, b and c (without inhibitors) and a*, b* and c* (doped with blend A wax inhibitor at 1000 - ppm) at 15 °C.

eight blended inhibitors at varying temperatures (0–50°*C*) and constant concentration (1500 ppm) and shear rate (120 1/s). An improved performance was observed in Blend 'A' sample, which provided the highest inhibition in decreasing the crude oil viscosity, wax appearance temperature, and pour point. For instance, at 5°*C*, blend 'A' wax inhibitor reduces the viscosity of undoped crude oil (i.e., without inhibitor) shown in Fig. 16 from 5 Pa s to 0.35 Pa s shown in Fig. 17. This value is lower than the viscosity of 0.53 Pa s achieved by the W2001 inhibitor, the best inhibitor among the four original samples.

On the other hand, the pour point and WAT of undoped crude oil reduced from 25.5°*C* and 30°*C* to 13.5°*C*and 18°*C*, respectively, as the crude oil is doped with blend A inhibitor. As such, the depositional issue could be avoided at or above the later temperature envelope. Hence, blended A provides better structural interference for the crystal nucleation, agglomeration, and growth within the oil matrix, thereby produces improved inhibition performance compared to the other tested inhibitors.

E.Microscopic analysis of crude oil

Fig. 18 compares the microscopic structures of crude oil samples A, B, and C at 0 ppm (undoped oil) with those of doped with blended 'A' inhibitor at 1000-ppm. The strong interlocking and interactions between the wax crystals are observed in the undoped samples. Clear needle-shaped crystal structures (platelets viewed on-edge by the microscope) are seen in the three crude oil samples (Fig. 18a and b and c) that cross-linked to form 3D structures. This assembled crystals network is the source of gel formation (Coto et al., 2014). Amongst these samples, crude oil B displayed a much more robust network of the wax crystal structure. These confirmed the presence of higher dense crystals in sample B, followed by A and then C. This behaviour is evidence by the amount of wax content in each sample shown in Table 1.

The addition of blend A PPD in different oil both resulted in distorted and smaller crystals. The photomicrographs in Fig. 18 (sample a*, b*, and c*) shows that the presence of inhibitor has transformed the needle-shaped crystals into an agglomerate and small particles dispersed in the

oil matrix. However, the crystal network appeared denser in Fig. 8 (sample b*), with roundly shaped crystal clusters, which could explain that the resulting wax content in the sample is higher, and the sample requires higher dynamic yield strength than sample a* and c*. Although the crystal dimensions were shown to be smaller than without additive, higher asphaltene in a* and c* led to the formation of small and finely dispersed wax crystals. Similar behaviour was reported by Ruwoldt et al. (2019). The new inhibitor effectively disrupted the strong interactions of the wax crystals around the microsphere, inhibiting the development of wax crystal network structure.

5. Conclusion

Three crudes oil samples and four Polymer-based pour point depressants were successfully studied using both established techniques and modified approaches. A summary of the findings is as follows:

- The oil samples are found as highly paraffinic oils based on the analysis of their fundamental properties and features such as the wax content, SARA fraction, n-Paraffin distribution, viscosity, macroscopic crystal morphology, CII, WAT, and pour point. The wax content in each sample is sufficient to entrap the liquid phase, which leads to an increase in oil viscosity or, in some cases, gels crude oil molecules. The photomicrographs of wax crystals in crude oil and other properties such as pour point and WAT revealed the complex nature of the undoped oil samples with inhibitor. Sample 'B' oil was found to be more problematic than sample A and C even under ambient conditions.
- The effect of chemical inhibitors and their interaction on wax crystallization were studied through a comprehensive viscometric analysis and morphological characterisation. The pour point depressants showed different effects on WAT, PP, apparent viscosity, and crystal morphology. All the tested inhibitors effectively reduce the viscosity and delayed pour point and WAT of the crude oil. The effectiveness of the inhibitors varies based on their concentration and compositions. The additives' synergistic effect led to developing a new inhibitor (blend A), which performed better than initially tested chemicals. The new inhibitor promotes a transformation of wax crystal morphology towards smaller particles dispersed in the oil matrix and further reductions in apparent viscosity, WAT and PP compared to the other tested chemicals. This works sheds light on new inhibitor development by blending different inhibitors to promote performance synergies.

Credit author statement

Nura Makwashi, Conceptualization, Experimentation, Writing — original draft preparation. Donglin Zhao, Conceptualization, Writing – review & editing. Mukhtar Abdulkadir, Writing – review & editing. Tariq Ahmed, Writing – review & editing. Ishaka Muhammad, Experimentation, All authors have read and agreed to the published version of the manuscript.

Funding statement

This work was supported by Petroleum Technology development Fund (PTDF) a subsidiary of Nigeria National Petroleum Corporation (NNPC).

Declaration of competing interest

The authors declare no conflict of interest.

Acknowledgement

The authors would like to thank the Petroleum Technology Development Fund (PTDF) for its financial support and Roemex oil service company for the supply of crude oil samples and wax inhibitors.

References

Abdel-Waly, A.A., 1997. New correlation estimates viscosity of paraffinic stocks. Oil Gas J. 74 (34), 1–18. Available from: https://trid.trb.org/view/575291.

Adeyanju, O.A., Oyekunle, L.O., 2014. Influence of long chain acrylate ester polymers as wax inhibitors in crude oil pipelines. In: Proceeding of the Society of Petroleum Engineers (SPE) Annual International Conference and Exhibition, vols. 5–7. https://doi.org/10.2118/172844-MS.

Adeyanju, A.O., Oyekunle, L.O., Adeyanju, O., Oyekunle, L.O., 2013. Experimental study of wax deposition in a single phase sub-cooled oil pipelines. Nigeria Annual International Conference and Exhibition 167515. https://doi.org/10.2118/167515-MS.

Al-Safran, E.M., Brill, J.P., James, P., 2017. Applied Multiphase Flow in Pipes and Flow Assurance Oil and Gas Production. Available from: https://cds.cern.ch/record/2301024.

Al-yaari, M., 2011. Paraffin wax Deposition : mitigation & removal techniques. In: Spe 155412, pp. 14–16.

Alcazar-Vara, L.A., Buenrostro-Gonzalez, E., 2011. Characterisation of the wax precipitation in Mexican crude oils. Fuel Process. Technol. 92 (12), 2366–2374. https://doi.org/10.1016/j.fuproc.2011.08.012.

Allen, O.T., Roberts, P.A., 1978. Production Operations: Well Completions, Workover, and Stimulation, third ed., ume 2. Oil & Gas Consultants International, Inc, Tulsa.

American Petroleum Institute, 2011. Robust Summary of Information on Crude Oil, pp. 1–130. Available from: https://petroleumhpv.org/petroleum-substances-and-categories/~/media/89F496D8432545ABB06D85D0BD5D99D1.ashx.

Ashoori, S., Sharifi, M., Masoumi, M., Mohammad Salehi, M., 2017. The relationship between SARA fractions and crude oil stability. Egyptian Journal of Petroleum 26 (1), 209–213. https://doi.org/10.1016/j.ejpe.2016.04.002.

Asomaning, S., Watkinson, A.P., 2000. Petroleum stability and heteroatom species effects in fouling of heat exchangers by asphaltenes. Heat Tran. Eng. 21 (3), 10–16. https://doi.org/10.1080/014576300270852.

Bai, Y., Bai, Q., 2005. Wax and Asphaltenes, Subsea Pipelines and Risers, first ed. ELSEVIER, Great Britain. https://doi.org/10.1016/B978-008044566-3.50023-3.

Bai, C., Zhang, J., 2013. Thermal, macroscopic, and microscopic characteristics of wax deposits in field pipelines. Energy Fuels 27 (2), 752–759. https://doi.org/10.1021/ef3017877.

Chanda, D., Sarmah, A., Borthakur, A., Rao, K.V., Subrahmanyam, B., Das, H.C., 1998. Combined effect of asphaltenes and flow improvers on the rheological behaviour of Indian waxy crude oil. Fuel 77 (11), 1163–1167. https://doi.org/10.1016/S0016-2361(98)00029-5.

Chi, Y., Daraboina, N., Sarica, C., 2016. Investigation of inhibitors efficacy in wax deposition mitigation using a laboratory scale flow loop. AIChE J. 62 (11), 4131–4139. https://doi.org/10.1002/aic.15307.

Cochran, S., 2003. Hydrate control and remediation best practices in deepwater oil developments. In: Offshore Technology Conference, pp. 179–192.

Coto, B., Coutinho, J.A.P., Martos, C., Robustillo, M.D., Espada, J.J., Peña, J.L., 2011. Assessment and improvement of n -paraffin distribution obtained by HTGC to predict accurately crude oil cold properties. Energy Fuels 25 (3), 1153–1160. https://doi.org/10.1021/ef101642g.

Coto, B., Martos, C., Espada, J.J., Robustillo, M.D., Peña, J.L., 2014. Experimental study of the effect of inhibitors in wax precipitation by different techniques. Energy Science and Engineering 2 (4), 196–203. https://doi.org/10.1002/ese3.42.

de Oliveira, M., Vieira, L., Miranda, L., Miranda, D., Marques, L.C.C., 2016. On the influence of micro-and macro-cristalline paraffins on the physical and rheological properties of crude oil and organic solvents. Chemistry and Chemical Technology 10 (4), 451–458. https://doi.org/10.23939/chcht10.04.451.

Del Carmen García, M., Carbognani, L., Orea, M., Urbina, A., 2000. The influence of alkane class-types on crude oil wax crystallization and inhibitors efficiency. J. Petrol. Sci. Eng. 25 (3–4), 99–105. https://doi.org/10.1016/S0920-4105(99)00057-1.

Deshannavar, U.B., Rafeen, M.S., Ramasamy, M., Subbarao, D., 2010. Crude oil fouling: a review. J. Appl. Sci. 10 (24), 3167–3174.

Dickakian, G., Seay, S., 1988. Asphaltene precipitation primary crude exchanger fouling mechanism. Oil Gas J. 86 (10), 47–50.

Dobbs, J., 1999. A unique method of paraffin control in production operations. In: SPE Rocky Mountain Regional Meeting, 15-18 May, Gillette, Wyoming. Society of Petroleum Engineers (SPE).

Ekaputra, A.A., Sabil, K.M., Hosseinipo, A., Saaid, I. Bin, 2014. Impacts of viscosity, density and pour point to the wax deposition. J. Appl. Sci. 14 (23), 3334–3338. https://doi.org/10.3923/jas.2014.3334.3338.

Erceg Kuzmić, A., Radošević, M., Bogdanić, G., Srića, V., Vuković, R., 2008. Studies on the influence of long chain acrylic esters polymers with polar monomers as crude oil flow improver additives. Fuel 87 (13–14), 2943–2950. https://doi.org/10.1016/J.FUEL.2008.04.006.

Fan, T., Buckley, J.S., 2002. Rapid and accurate SARA analysis of medium gravity crude oils. Energy Fuels 16 (6), 1571–1575. https://doi.org/10.1021/ef0201228.

Fan, T., Wang, J., Buckley, J.S., 2002. Evaluating crude oils by SARA analysis. In: SPE/DOE Improved Oil Recovery Symposium, 4 2002. Society of Petroleum Engineers (SPE), pp. 883–889.

França, D., Pereira, V.B., Coutinho, D.M., Ainstein, L.M., Azevedo, D.A., 2018. Speciation and quantification of high molecular weight paraffins in Brazilian whole crude oils

using high-temperature comprehensive two-dimensional gas chromatography. Fuel 234, 1154–1164. https://doi.org/10.1016/J.FUEL.2018.07.145.
Halim, N., Ali, S., Nadeem, M., Hamid, P.A., Tan, I.M., 2011. Synthesis of wax inhibitor and assessment of squeeze technique application for Malaysian waxy crude. Available from: http://eprints.utp.edu.my/8792/1/SPEnadhirah.pdf.
Hammami, a, Ratulowski, J., 2007. Precipitation and Deposition of Asphaltenes in Production Systems: A Flow Assurance Overview, *Asphaltenes, Heavy Oils, and Petroleomics*, pp. 617–660. https://doi.org/10.1007/0-387-68903-6_23.
Hao, L.Z., Al-salim, H.S., Ridzuan, N., 2019. A review of the mechanism and role of wax inhibitors in the wax deposition and precipitation. Pertanika J. Sci. & Technol 27 (1), 499–526.
Hasinger, M., Scherr, K.E., Lundaa, T., Bräuer, L., Zach, C., Loibner, A.P., 2012. Changes in iso- and n-alkane distribution during biodegradation of crude oil under nitrate and sulphate reducing conditions. J. Biotechnol. 157 (4), 490–498. https://doi.org/10.1016/j.jbiotec.2011.09.027.
Hoffmann, R., Amundsen, L., 2010. Single-phase wax deposition experiments. Energy Fuels 24 (2), 1069–1080. https://doi.org/10.1021/ef900920x.
Hoffmann, R., Amundsen, L., 2013. Influence of wax inhibitor on fluid and deposit properties. J. Petrol. Sci. Eng. 107, 12–17. https://doi.org/10.1016/j.petrol.2013.04.009.
Holder, G.A., Winkler, J., 1965. Crystal-growth poisoning of n-paraffin wax by polymeric additives and its relevance to polymer crystallization mechanisms. Nature 207 (4998), 719–721. https://doi.org/10.1038/207719a0.
Huang, Z., Zheng, S., Fogler, H., 2015. Wax Deposition: Experimental Characterisations, Theoretical Modeling, and Field Practices. CRC Press. https://doi.org/10.1201/b18482.
Japper-Jaafar, A., Bhaskoro, P.T., Mior, Z.S., 2016. A new perspective on the measurements of wax appearance temperature: comparison between DSC, thermomicroscopy and rheometry and the cooling rate effects. J. Petrol. Sci. Eng. 147, 672–681. https://doi.org/10.1016/j.petrol.2016.09.041.
Jennings, D.W., Newberry, M.E., 2008. Paraffin inhibitor applications in deepwater offshore developments. In: International Petroleum Technology Conference, IPTC *2008*, vol. 2, pp. 834–847.
Jewell, D.M., Weber, J.H., Bunger, J.W., Plancher, H., Latham, D.R., 1972. Ion-exchange, coordination, and adsorption chromatographic separation of heavy-end petroleum distillates. Anal. Chem. 44 (8), 1391–1395. https://doi.org/10.1021/ac60316a003.
Jha, N.K., Jamal, M.S., Singh, D., Prasad, U.S., 2014. Characterisation of crude oil of upper Assam field for flow assurance. In: Society of Petroleum Engineers - SPE Saudi Arabia Section Technical Symposium and Exhibition.
Kang, P.-S., Lee, D.-G., Lim, J.-S., 2014. Status of wax mitigation technologies in offshore oil production. The Twenty-Fourth International Ocean and Polar Engineering Conference 3, 31–38. Available from: www.isope.org.
Kasumu, A.S., 2014. An Investigation of Solids Deposition from Two-phase Wax-Solven-Water Mixtures. Doctoral thesis, University of Calgary, Calgary, AB.
Keeper, G., 2013. Paraffin Wax : Formation , Mitigation Methods & Remediation Techniques. Gibson Applied technology and Engineering, Inc. Available from: http://static1.squarespace.com/static/53556018e4b0fe1121e112e6/54b683d0e4b09b2abd348a7b/54b683e1e4b09b2abd348dbe/1421247457412/GAT2004-GKP-2013.04-Paraffin-Formation-Mitigation-and-Remediation-Techniques.pdf?format=original.
Kelland, M.A., 2009. Production Chemicals for the Oil and Gas Industry, Production Chemicals for the Oil and Gas Industry. CRC Press. https://doi.org/10.1201/9781420092974.
Kok, M.V., Saracoglu, R.O., 2000. Mathematical modelling of wax deposition in crude oil pipelines (comparative study). Petrol. Sci. Technol. 18 (9–10), 1121–1145. https://doi.org/10.1080/10916460008949895.
Lab, K.A.T., 2009. HTGC METHOD NOTES - T-SEP®. Kernow Instrument Technology. Accessed 13 March 2017. http://www.kat-lab.com/t-sep/tsep2.html. http://www.kat-lab.com/t-sep/index.html.
Lee, H.S., 2008. Computational and Rheological Study of Wax Deposition and Gelation in Subsea Pipelines. Doctoral dissertation, University of Michigan.
Li, N., Mao, G.L., Shi, X.Z., Tian, S.W., Liu, Y., 2018. Advances in the research of polymeric pour point depressant for waxy crude oil. J. Dispersion Sci. Technol. 39 (8), 1165–1171. https://doi.org/10.1080/01932691.2017.1385484.
Makwashi, N., 2020. Investigation of Wax Depositional Behaviour in Straight and Curved Pipes – Experiments and Simulation. PhD Thesis. London South Bank University.
Makwashi, N., Soraia, D., Barros, D., Sarkodie, K., Zhao, D., Diaz, P.A., 2019. Depositional behaviour of highly macro-crystalline waxy crude oil blended with polymer inhibitors in a pipe with a 45-degree bend. In: Society of Petroleum Engineers SPE-195752-MS.
Mansoori, G.A., 2009. A unified perspective on the phase behaviour of petroleum fluids. Int. J. Oil Gas Coal Technol. 2 (2), 141–167. https://doi.org/10.1504/IJOGCT.2009.024884.
Mozes, G.E., 1982. Paraffin Products: Properties, Technologies, Applications, *Developments in Petroleum Science*. Elsevier Science & Technology.
Nguyen, D.A., Fogler, H.S., 2005. Facilitated diffusion in the dissolution of carboxylic polymers. AIChE J. 51 (2), 415–425. https://doi.org/10.1002/aic.10329.
Nguyen, D.A., Scott Fogler, H., Chavadej, S., 2001. Fused chemical reactions. Encapsulation: Application to Remediation of Paraffin Plugged Pipelines † 2 https://doi.org/10.1021/ie0009886.
Paar, Anton, 2020. Rheological investigation of petrochemicals. Available from: https://wiki.anton-paar.com/en/basics-of-rheology/rheological-investigation-of-petrochemicals/#c49283.
Paso, K.G., 2014. Comprehensive treatise on shut-in and restart of waxy oil pipelines. J. Dispersion Sci. Technol. 35 (8), 1060–1085. https://doi.org/10.1080/01932691.2013.833105.
Pedersen, K.S., Rønningsen, H.P., 2003. Influence of wax inhibitors on wax appearance temperature, pour point, and viscosity of waxy crude oils. Energy Fuels 17 (2), 321–328. https://doi.org/10.1021/ef020142+.
Perez, P., Boden, E., Chichak, K., Gurnon, A.K., Hu, L., Lee, J., et al., 2015. Evaluation of Paraffin Wax Inhibitors: an Experimental Comparison of Bench-Top Test Results and Small-Scale Deposition Rigs for Model Waxy Oils. Offshore Technology Conference, pp. 4–7. https://doi.org/10.4043/25927-MS. Proceedings.
Ragunathan, T., Husin, H., Wood, C.D., 2020. Wax formation mechanisms , wax chemical inhibitors and factors affecting chemical inhibition. Appl. Sci. 10 (2), 479. https://doi.org/10.3390/app10020479.
Rehan, M., Nizami, A.S., Taylan, O., Al-Sasi, B.O., Demirbas, A., 2016. Determination of wax content in crude oil. Petrol. Sci. Technol. 34 (9), 799–804. https://doi.org/10.1080/10916466.2016.1169287.
Rodriguez-Fabia, S., Lopez Fyllingsnes, R., Winter-Hjelm, N., Norrman, J., Paso, K.G., 2019. Influence of measuring geometry on rheomalaxis of macrocrystalline wax-oil gels: alteration of breakage mechanism from adhesive to cohesive. Energy Fuels 33 (2), 654–664. https://doi.org/10.1021/acs.energyfuels.8b02725.
Roenningsen, H.P., Bjoerndal, B., Baltzer Hansen, A., Batsberg Pedersen, W., 1991a. Wax precipitation from North Sea crude oils: 1. Crystallization and dissolution temperatures, and Newtonian and non-Newtonian flow properties. Energy Fuels 5 (6), 895–908. https://doi.org/10.1021/ef00030a019.
Ruwoldt, J., Kurniawan, M., Oschmann, H.-J.J., 2018. Non-linear dependency of wax appearance temperature on cooling rate. J. Petrol. Sci. Eng. 165, 114–126. https://doi.org/10.1016/j.petrol.2018.02.011.
Ruwoldt, J., Sørland, G.H., Simon, S., Oschmann, H., Sjöblom, J., 2019. Inhibitor-wax interactions and PPD effect on wax crystallization : new approaches for GC/MS and NMR , and comparison with DSC , CPM , and rheometry. J. Petrol. Sci. Eng. 177 (February), 53–68. https://doi.org/10.1016/j.petrol.2019.02.046.
Sarica, C., Panacharoensawad, E., 2012. Review of paraffin deposition research under multiphase flow conditions. Energy Fuels 26 (7), 3968–3978. https://doi.org/10.1021/ef300164q.
Sifferman, T.R., 1979. Flow properties of difficult-to-handle waxy crude oils. J. Petrol. Technol. 31 (8), 1042–1050. https://doi.org/10.2118/7409-PA.
Siljuberg, M.K., 2012. Modelling of Paraffin Wax in Oil Pipelines. Norwegian University of Science and Technology. Available from: : https://ntnuopen.ntnu.no/ntnu-xmlui/handle/11250/239864.
Singh, P., Fogler, H.S., 1998. Fused chemical reactions: the use of dispersion to delay reaction time in tubular reactors. Ind. Eng. Chem. Res. 37 (6), 2203–2207. https://doi.org/10.1021/ie9706020.
Singh, A., Lee, H.S., Singh, P., Sarica, C., 2011. SS: flow assurance: validation of wax deposition models using field data from a subsea pipeline. In: Offshore Technology Conference, pp. 2–5.
Sousa, A.L., Matos, H.A., Guerreiro, L.P., 2019. Preventing and removing wax deposition inside vertical wells: a review. J. Petrol. Explor. Prod. Technol. 9, 2091–2107. https://doi.org/10.1007/s13202-019-0609-x.
Theyab, M.A., Diaz, P., 2016a. Experimental study of wax deposition in pipeline – effect of inhibitor and spiral flow. International Journal of Smart Grid and Clean Energy 174–181. https://doi.org/10.12720/sgce.5.3.174-181.
Theyab, M., Diaz, P., 2016b. Experimental study on the effect of inhibitors on wax deposition. J. Petrol Environ. Biotechnol. 7 (6) https://doi.org/10.4172/2157-7463.1000310.
Turner, W., 1971. Normal alkanes. Ind. Eng. Chem. Prod. Res. Dev. 10 (3), 238–260. https://doi.org/10.1021/i360039a003.
Wang, J., Buckley, J., 2002. Standard Procedure for Separating Asphaltenes from Crude Oils. New Mexico Tech, PRRC, p. 2.
Wang, W., Huang, Q., Wang, C., Li, S., Qu, W., Zhao, J., He, M., 2015. Effect of operating conditions on wax deposition in a laboratory flow loop characterized with DSC technique. J. Therm. Anal. Calorim. 119 (1), 471–485. https://doi.org/10.1007/s10973-014-3976-z.
Wang, Z., Yu, X., Li, J., Wang, J., Zhang, L., 2016. The use of biobased surfactant obtained by enzymatic syntheses for wax deposition inhibition and drag reduction in crude oil pipelines. Catalysts 6 (5), 61. https://doi.org/10.3390/catal6050061.
Wayne, C., Sue, D., 2015. Agilent Collaborates with University to Solve Significant Problem for Oil Refineries. *Agilent*. Available from: https://www.agilent.com/en-us/newsletters/accessagilent/2015/jul/sara?cid=11649.
Woo, G.T., Garbis, S.J., Gray, T.C., 1984. Long-term control of paraffin deposition. In: Proceedings - SPE Annual Technical Conference and Exhibition. Society of Petroleum Engineers (SPE).
Wu, Y., Ni, G., Yang, F., Li, C., Dong, G., 2012. Modified maleic anhydride co-polymers as pour-point depressants and their effects on waxy crude oil rheology. Energy Fuels 26 (2), 995–1001. https://doi.org/10.1021/ef201444b.
Yang, F., Li, C., Yang, S., Zhang, Q., Xu, J., 2014. Effect of dodecyl benzene sulfonic acid (DBSA) and lauric amine (LA) on the associating state and rheology of heavy oils. J. Petrol. Sci. Eng. 124, 19–26. https://doi.org/10.1016/J.PETROL.2014.10.004.
Yang, F., Zhao, Y., Sjöblom, J., Li, C., Paso, K.G., 2015. Polymeric wax inhibitors and pour point depressants for waxy crude oils: a critical review. J. Dispersion Sci. Technol. 36 (2), 213–225. https://doi.org/10.1080/01932691.2014.901917.
Yen, A., Yin, Y.R., Asomaning, S., 2001. Evaluating asphaltene inhibitors: laboratory tests and field studies. SPE International Symposium on Oilfield Chemistry. https://doi.org/10.2118/65376-MS.
Zeng, H., Zou, F., Lehne, E., Zuo, J.Y., Zhang, D., 2012. Advanced Gas Chromatography - Progress in Agricultural. Biomedical and Industrial Applications. https://doi.org/10.5772/2518.

Zheng, S., Saidoun, M., Mateen, K., Palermo, T., Ren, Y., Fogler, H.S., 2016. Wax Deposition Modeling with Considerations of Non-newtonian Fluid Characteristics. Offshore Technology Conference, p. 20. https://doi.org/10.4043/26914-MS.

Zheng, S., Saidoun, M., Palermo, T., Mateen, K., Fogler, H.S., 2017. Wax deposition modeling with considerations of non-Newtonian characteristics: application on field-scale pipeline. Energy Fuels 31 (5), 5011–5023. https://doi.org/10.1021/acs.energyfuels.7b00504.

Zhu, T., Walker, J. a, Liang, J., Laboratory, P.D., 2008. Evaluation of Wax Deposition and its Control during Production of Alaska North Slope Oils. https://doi.org/10.2172/963363.